Distributed Parameter Estimation for Complex Energy Systems

by

Janak Agrawal
B.S. Electrical Engineering and Computer Science
Massachusetts Institute of Technology, 2019

Submitted to the Department of Electrical Engineering and Computer Science
in partial fulfillment of the requirements for the degree of

Master of Engineering in Electrical Engineering and Computer Science

at the

MASSACHUSETTS INSTITUTE OF TECHNOLOGY

September 2020

Author .....
Department of Electrical Engineering and Computer Science
August 10, 2020

Certified by .....
Marija Ilic
Senior Research Scientist
Thesis Supervisor

Accepted by .....
Katrina LaCurts
Chair, Master of Engineering Thesis Committee

Distributed Parameter Estimation for Complex Energy Systems

by

Janak Agrawal

B.S. Electrical Engineering and Computer Science

Massachusetts Institute of Technology, 2019

Submitted to the Department of Electrical Engineering and Computer Science
on August 10, 2020, in partial fulfillment of the
requirements for the degree of
Master of Engineering in Electrical Engineering and Computer Science

Abstract

With multiple energy sources, diverse energy demands, and heterogeneous socioeconomic factors, energy systems are becoming increasingly complex. Multifaceted components have non-linear dynamics and are interacting with each other as well as the environment. In this thesis, we model components in terms of their own internal dynamics and output variables at the interfaces with the neighboring components.

We then propose to use a distributed estimation method for obtaining the parameters of the the component's internal model based on the measurements at its interfaces. We check whether theoretical conditions for distributed estimation approach are met and validate the results obtained. The estimated parameters of the system can then be used for advanced control purposes in the HVAC system.

We also use the measurements at the terminals to model and verify the components in the energy-space which is a novel approach proposed by our group. The energy space approach reflects conservation of power and rate of change of reactive power. Both power and rate of change of generalized reactive power are obtained from measurements at the input and output ports of the components by measuring flows and efforts associated with their ports. A pair of flow and efforts is measured for electrical and gas ports, as well as for fluids. We show that the energy space model agrees with the conventional state space model with a high accuracy and that standard measurements available in a commercial HVAC can be used for calculating the interaction variables in the energy space model.

A novel finding is that unless measurements of both flow and effort variables is used, the sub-model representing rate of change of reactive power can not be validated. This implies that commonly used models in engineering which assume constant effort variables may not be sufficiently accurate to support most efficient control of complex interconnected systems comprising multiple energy conversion processes.

Thesis Supervisor: Marija Ilic
Title: Senior Research Scientist

Acknowledgments

I would first like to express my utmost gratitude to my supervisor Prof. Ilic without whose support this thesis would not have come to fruition. Her guidance and constant feedback has been essential throughout my Masters in keeping me motivated and producing a high quality of work.

I would also like to thank my group at LIDS at MIT and it has been a great learning experience working with my co-researchers. I would like to thank Pallavi Bharadwaj for the encouragement and valuable input in my work. I am also grateful to Dan Wu, Anna Jevtic and Rupamathi Jaddivada whose previous work has been essential for this thesis. The immense progress that we have made in this project is a result of the productive collaboration and efficient team work amongst our group. Thank you for the constant support and fun conversations.

I also appreciate all the help received from Mike Gao, Min Zhang, Le Li, Jinyi Zhang and others at ENN Science and Technology Development. Thank you for sponsoring my Masters as a part of Dynamic Monitoring and Decision Systems (DyMonDS) Framework for IT-enabled Engineering of Retail-level Energy Services (RES) project (MIT Reference: 6940611). This wouldn't have been possible without your help and collaboration. I am grateful for your hard work and thoughtfulness in providing us with the information we needed.

Last but not the least, I would like to thank MIT CSAIL and MIT Energy Initiative for giving me this opportunity and all the administrators/staff who helped me stay on track during my Masters.

Contents

List of Figures

List of Tables

Chapter 1

Introduction

1.1 Motivation

With the growing demand of energy worldwide, there is a real urgency for developing more intelligent energy systems, especially ones that can be implemented today. With multiple energy sources and diverse energy demands, energy systems are becoming increasingly complex and multifaceted. For example, in this thesis we consider a complex heating-ventilation-air conditioning (HVAC) systems which consists of several components with non-linear dynamics including water, gas, electricity and air networks interacting with each other as well as the environment. Therefore, it is becoming challenging to improve the efficiency of such complex systems without improving upon the existing techniques used for mapping and controlling these systems. To address these challenges, we propose a novel approach to mapping and monitoring integrated energy systems.

HVAC's are extensively used in household as well as commercial building and account for 30% of the total electricity consumption in buildings in US [19]. The majority of HVAC controllers still operate on old-age classical methodologies which are often based on pre-programmed logic [36]. However, more advanced control strategies like model predictive control (MPC) [10] [26] or adaptive control [27] [37], which are harder to implement, can more efficiently track the heating/cooling load of the building, thus, reducing the overall energy consumption of a building [11] [12]. These

advanced strategies require basic knowledge of system model, which is generally complex, interconnected and has unknown parameters. Therefore, we need an estimator which is responsible for calculating the unknown parameters of the system using prior knowledge as well as real-time measurements. The output of the estimator is given to the control and the accuracy of the control is directly dependent on the accuracy of the estimator. To further improve state-of-the-art system control algorithms we need to advance state estimation of complex systems.

This thesis also concerns with the difficult problem of managing complex interconnected dynamical systems. With the growing energy demand, energy systems in the future will be more complex comprising heterogeneous sub-components involving multi-energy conversions. Overcoming the complexity of modelling these systems is essential for efficient energy-conversion control. Therefore, we utilize a novel modeling to derive an aggregate, low-order, dynamical model of these components [22] [25].

1.2 State of the Art

Designing efficient control for a complex system requires knowledge about the empirical parameters of the components of the system. Traditionally these empirical parameters have been estimated by employing expensive sensors such as mass flow meters. But use of mass flow meters in every case is not possible which may lead to a badly tuned model. To avoid this problem, modern controllers rely on experimental mappings between the desired outputs, and the power consumed by the controllers, much the same way as in frequency regulation one relies on generator droops [29] [21]. Their performance depends on the internal dynamics of equipment and their feedback control. The main challenge is how to increase efficiency without requiring complex fast fail-prone communications while having only limited measurements for control.

This problem is even more tangible in large interconnected systems. While the structure of these large interconnected systems is extensively studied, the question concerning the decomposition of the interconnected system while taking into account

the availability of measurements and control is rarely studied. In this thesis we take a general large-scale dynamical systems point of view and recall conditions under which a complex system can be decomposed into subsystems whose local measurements are sufficient for distributed parameter estimation. We use real world measurement data to show that such a decomposition works well for the HVAC system under consideration and can be key to determining unknown parameters of large dynamical energy systems. To the best of our knowledge, this question has not been addressed in the previous literature of large-scale dynamical systems.

From the systems perspective, traditionally power grids have been studied by utilizing Thevenin and Norton's equivalent circuits recomputed every timestep, the accuracy of which depends on the chosen interaction protocols and are generally not scalable to very large systems. This has been a valid approach in the past when the disturbances entering the grid such as those from the renewables and did not form a high fraction of the generation portfolio. Typically, the benchmark problems for the energy management are non-convex. To apply any decomposition strategy, these constraints are all simplified by applying convex approximations. These approaches, however, are not scalable [22] [25]. Here, we verify a novel energy-power modelling approach which uses effort and flow variables at interfaces to design aggregate models of complex systems in multi-energy domains. We use this approach to show that it can be easily applied to a commercial HVAC system and hence be used to account for the complexity of a commercial HVAC system and can help design controllers which can respond to fast-response disturbances which are often ignored in conventional state space controllers.

1.3 Contribution

The main objective of this thesis has been to perform distributed parameter estimation in complex dynamical systems using only available measurements.

Majority of literature regarding parameter estimation for power systems has been focused on a single component fixed to a test bench. In this thesis, we tackle the issue

of distributed parameter estimation for an interconnected system using measurement data from a real world HVAC system.

The energy-power space was introduced for modeling interactions in multi-energy systems using aggregate interaction variables. It was shown that real power and generalized reactive power can be defined for any type of energy system by using analogies for efforts and flows. They represent interaction variables whose dynamical models are sufficient to model input-output characteristics of components and their interactions within the complex system. This modelling was originally derived for electrical systems and has been proved for several electrical devices [23] [22]. In this thesis, for the first time, we verify the energy-power space model of an industrial chiller using sensor measurement. Such an approach has never been used before to model a component in a commercial HVAC.

This thesis addresses some of the most prominent issues regarding models and their parameters still challenging the design of efficient controls for HVACs. In this thesis we use an HVAC system to verify our methodology but its versatility in being applicable to a huge array of systems opens up a lot of possibilities for future smart controllers.

1.4 Outline

The remainder of the thesis is outlined as follows:

Chapter 2 provides an overview and component level description of the HVAC system under consideration. We also provide a brief background on the work that this paper builds upon.

Chapter 3 discusses previous work done in this field of research and their effectiveness.

Chapter 4 describes the approach used to model the components and estimate unknown parameters in the HVAC system.

Chapter 5 describes the tools used to implement the approach in Chapter 4.

Chapter 6 states the numerical results obtained using the methodology specified

in Chapter 4.

Chapter 7 concludes with the contributions of this thesis and future work.

1.5 List of Publications

These publications formulated during the Masters project are the core of this thesis:

1. P. Bharadwaj, J. Agrawal, R. Jaddivada, M. Zhang and M. Ilic. Measurement-based Validation of Energy-Space Modelling in Multi-Energy Systems.

   Submitted to 2020 North American Power Symposium (NAPS).

2. D. Wu, J. Agrawal, P. Bharadwaj, L. Li, J. Zhang and M. Ilic. On The Validity of Decomposition for Distributed Parameter Estimation in Complex Dynamical Systems: The Case of Cooling Systems.

   Submitted to 2020 North American Power Symposium (NAPS).

Chapter 2

Background

2.1 Description of HVAC system

For this thesis, we have used data from a real-world HVAC system that offers heating, cooling and power to a commercial building over the year. The HVAC system consists of electricity, gas, airflow and waterflow networks as its main components which can also be seen in Fig. 2-1. A more detailed sketch of the same HVAC system can be seen in Fig. 2-3. We can see the flow of different forms of energy such as gas and electricity in these figures and how the various networks interact with each other.

This is a complex HVAC system with a cooling capacity of 500 MW, heating capacity of 500MW and power generation capacity of 40 MW. Here we provide a brief description of all the components that are present in this HVAC system and also analyse the flow of energy from one component to another.

2.1.1 Components of HVAC

Although, the HVAC contains several components, small and big, which are essential for its functioning, here we focus on a few major components of the HVAC which consume the most energy and are also studied upon in the rest of the thesis. A detailed sketch of all the components can be found in Fig. 2-3, whereas, a simplified sketch of the components showing the measurements and control law of the components can

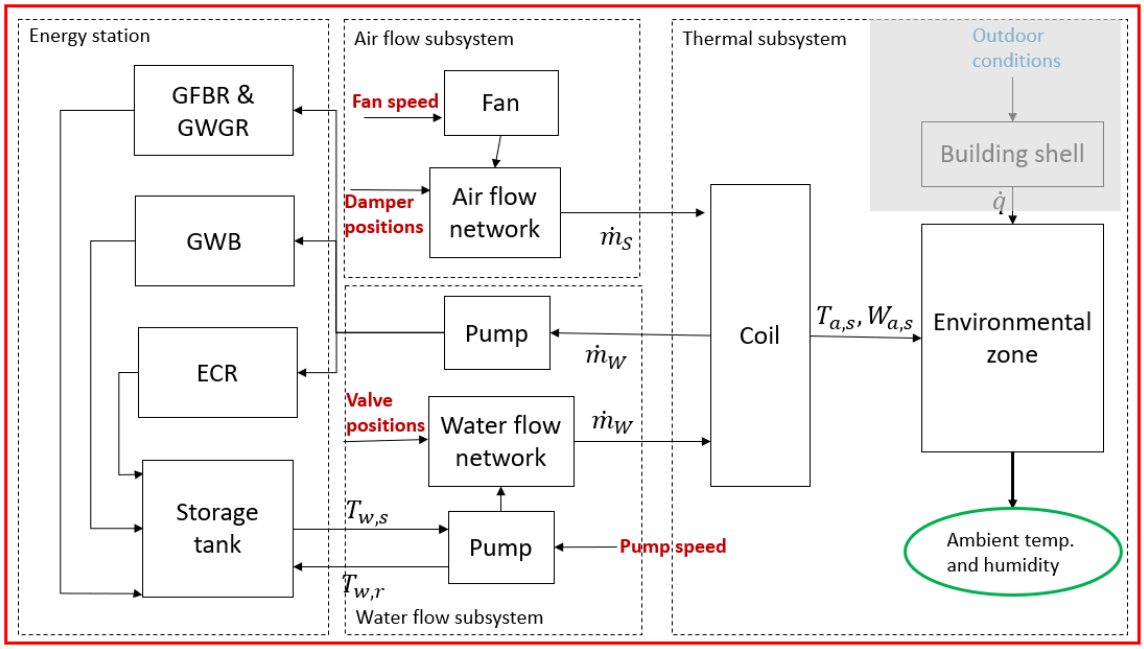

Figure 2-1: Decomposition of the full interconnected HVAC system into air flow,water flow and thermal subsystems

be found in 2-2.

Electric Chiller

An electric chiller, or more commonly known as centrifugal chiller, utilizes the vapor compression cycle to chill water and reject the heat collected from the chilled water plus the heat from the compressor to a second water loop cooled by a cooling tower [32]. We can see the sketch of the electric chiller in Fig. 2-2 (a).

Gas Chiller

A gas chiller also known as an absorption chiller consists of a evaporator, absorber, generator and heat exchanger. The chilled water is cooled down using a sudden change of pressure. First, the water is heated up in the generator which releases the water from the refrigerant and becomes vapor. Then, the vapor is transported to the evaporator where the low pressure cools down the water. Gas chillers can use different refrigerants like Li-Br or NH3-water. Since, they can operated using natural

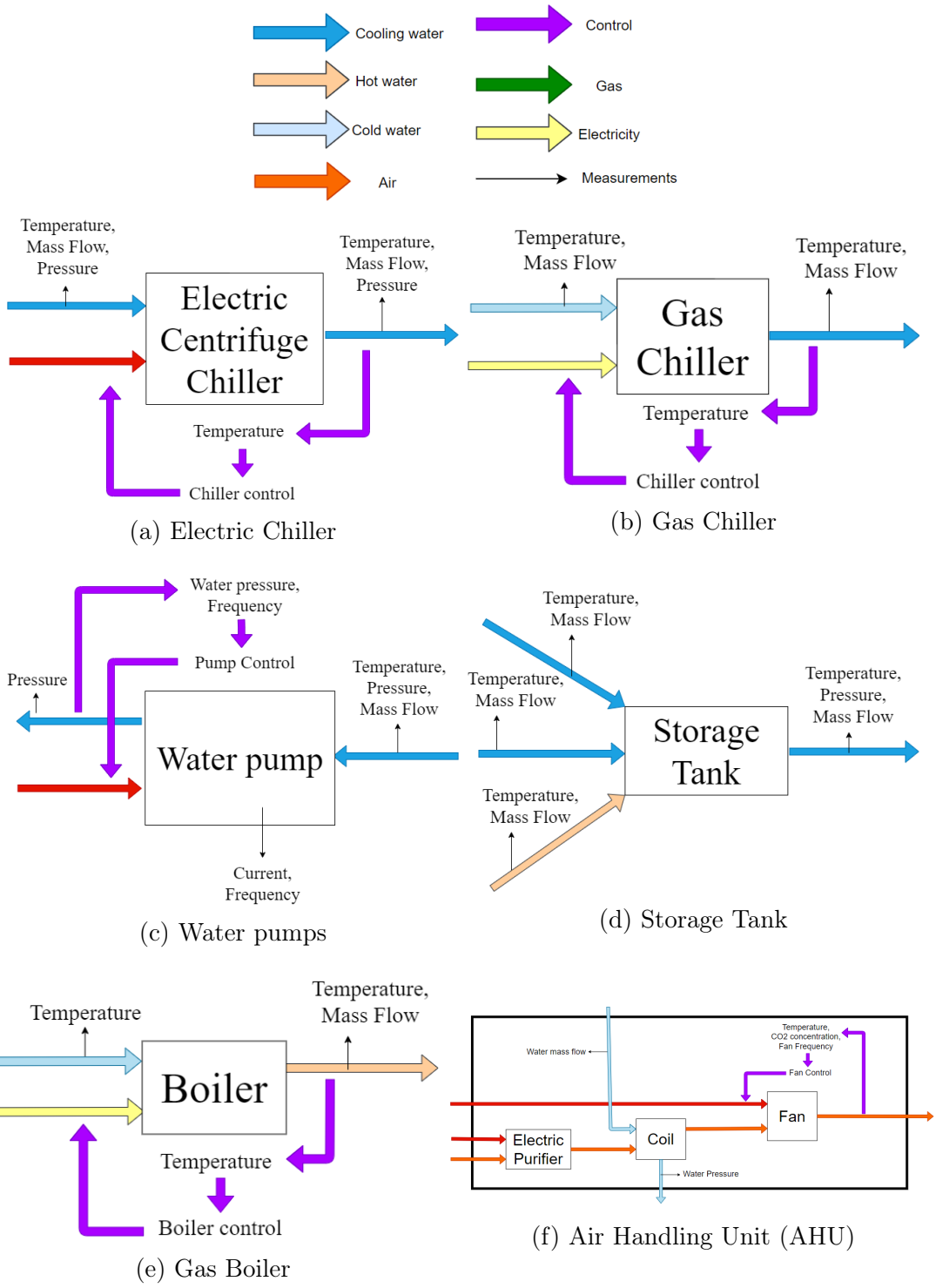

(a) Electric Chiller (b) Gas Chiller

(c) Water pumps (d) Storage Tank

(e) Gas Boiler (f) Air Handling Unit (AHU)

Figure 2-2: Multi-Energy flow model of commercial HVAC System [14]

gas or flue gases from other components, they are increasingly becoming common in commercial HVAC [15]. A diagram can be seen in Fig. 2-2 (b).

Water pumps

The water pumps used in this HVAC are centrifugal pumps which are placed along the water pipelines. There are two big arrays of water pumps, one for the water input of chillers and boilers, and other for the water input to the air-conditioning coils which can be seen in Fig. 2-3.

Storage Tank

A storage tank takes in the hot or cold water incoming from the chillers or boilers respectively and stores it until it needs to be transported to the air handling units.

Gas Boiler

The gas boiler burns natural gas and heats up the water supplied to it using the pumps. The output water is then stored in the storage tank.

Air Handling Unit

A commercial air handling unit or AHU consists of a fan, an electric purifier and a coil for hot/cool water. They take fresh ambient air from outside, clean it, heat or cool it and then transport it to a designated area of a building using ducts [9].

2.1.2 Thermal Subsystem

The thermal subsystem mainly consists of the coil (i.e. heat ex-changer), chillers, boilers, internal combustion generator (ICG) and thermal zones within the building shell.

In summers, the water is chilled to the desired temperature using the chillers and stored in a storage tank until delivered to the air-conditioning coils. The waste heat is discarded to the environment with the use of cooling towers shown in Fig. 2-3. In winters, the boiler and waste heat from ICG is used to heat up the water and pumped to the coil. The chillers and boilers are powered using electricity and gas bought from

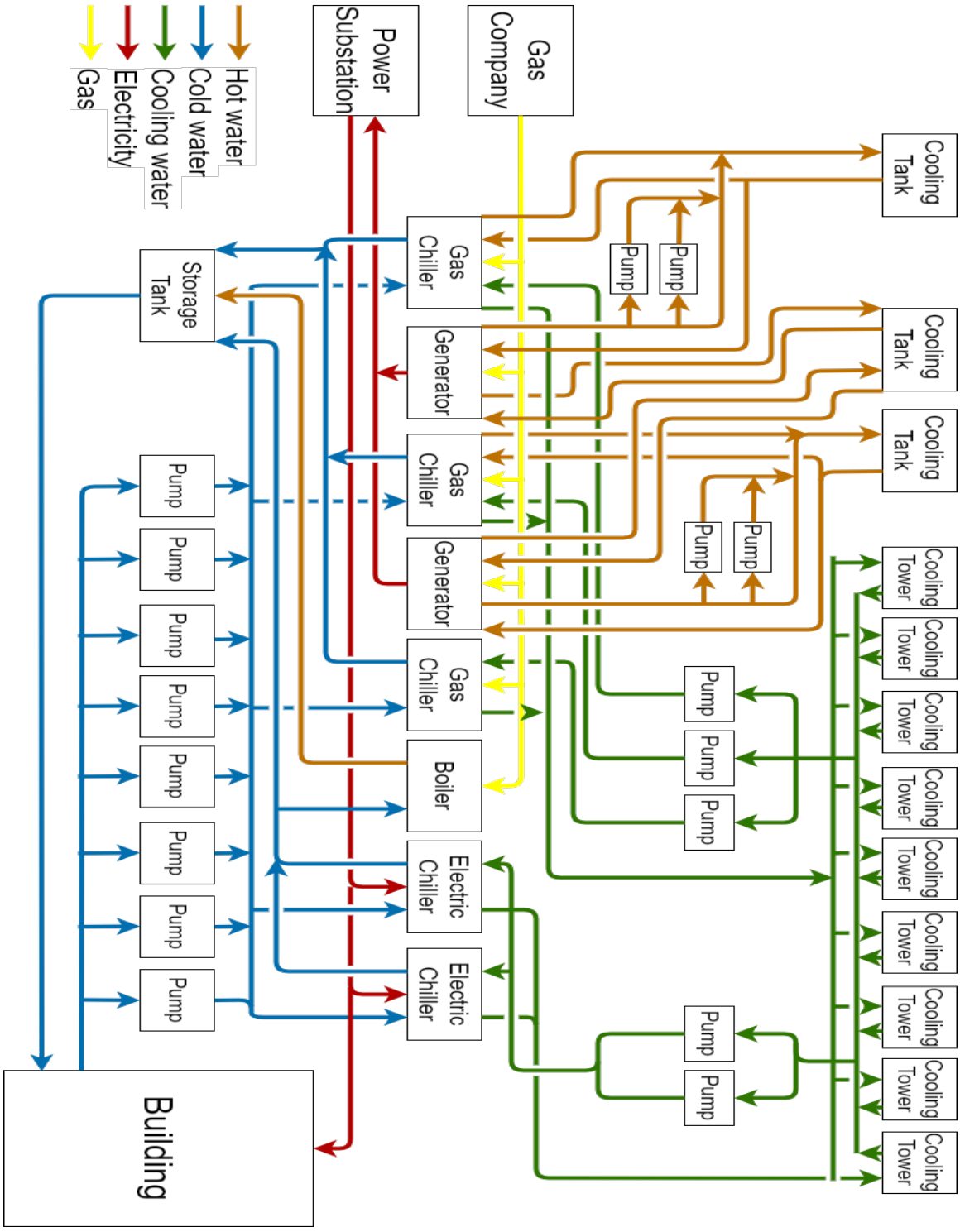

Figure 2-3: Multi-Energy flow model of commercial HVAC System

the state power grid and third-party company respectively. We provide a detailed analysis of energy consumption in thermal subsystem in Section 3.

2.1.3 Water Flow Subsystem

The waterflow subsystem is mainly comprised of the chillers, boilers, ICG, water pipeline network, water pumps, storage tank and the coil inside the air handling units (AHU).

Fresh and clean water is supplied by a third-party company which is then delivered to the chillers or boiler using the water pumps. Water is cooled or heated according to demand and is stored in the storage tank and delivered to AHUs using water pumps and a pipeline network as per demand.

2.1.4 Air Flow Subsystem

The air flow system consists of the AHUs inside the buildings and the coils.

The AHU takes in ambient air from outside and the temperature-controlled water inside the coils exchanges heat with the air and then, the cooled/heated air is then delivered to the respective thermal zone using ducts.

2.2 Gray Box System Identification

This section presents an approach at identifying system parameters of the HVAC using sensor measurements. For this purpose, many combinations and nuances of theoretical modeling from first principles and empirical modeling based on measurement data can be pursued. Basically, the following three different modeling approaches can be distinguished [28]:

1. White box models are those which can be derived directly from first principles and all parameters can be determined by theoretical modeling.

2. Black box models requires both model structure and parameters to be determined from experimental modeling.

3. Gray box models represent a compromise or combination between white and black box models. They are characterized by an integration of various kinds of information that are easily available.

Rarely we find pure white box or black box approaches in reality. Often the model structure may be determined by first principles but the model parameters may be estimated from data [20]. We use a similar approach in our analysis here and thus make use of gray box system identification techniques.

2.2.1 Non-linear least squares

Since we have no prior knowledge about the distribution of the parameters as well as the noise in the data, we assume that parameters are uniformly distributed over a given range and the noise is white with constant variance. Such a system can be efficiently identified using Non-Linear Least squares and optimized using Newtons method [28] [20].

For non-linear optimization algorithms, quadratic loss function is by far the most common in practice. If the parameters are linear, a least squares problem originates but for non-linear parameters, the loss $E(\theta)$ becomes,

$$\begin{aligned} E(\theta) &= \sum_{i=1}^{N} f^2(i,\theta) \qquad (2.1) \\ &= f^T f \\ where,\ f &= [f(1,\theta)\ ...\ f(N,\theta)]^T \qquad (2.2) \end{aligned}$$

and is known as non-linear least squares problem.

Let the modified Jacobian be,

$$J' = \begin{bmatrix} \delta f(1,\theta)/\delta\theta_1 & ... & \delta f(1,\theta)/\delta\theta_N \\ : & & : \\ \delta f(N,\theta)/\delta\theta_1 & ... & \delta f(N,\theta)/\delta\theta_N \end{bmatrix} \qquad (2.3)$$

The jth component of gradient of this loss function can be written as

$$g_j = \frac{\delta E(\theta)}{\delta \theta_j} = 2 \sum_{i=1}^{N} f(i,\theta) \frac{\delta f(i,\theta)}{\delta \theta_j} \tag{2.4}$$

Therefore, the gradient can be written as,

$$g = 2J^T f \tag{2.5}$$

2.2.2 Gauss-Newton Method

The Gauss-Newton method is the non-linear least squares version of the general Newtons method [28].

the goal of optimization is that each iteration step should decrease the loss function value, i.e., $E(\theta_k) < E(\theta_{k-1})$. For a general gradient-based optimization, the principle is to change the parameter vector θ proportional to some step size η_{k-1} into a direction p_{k-1}:

$$\theta_k = \theta_{k-1} - \eta_{k-1} * p_{k-1} \tag{2.6}$$

The vector p_k for Newtons method is given by,

$$p_k = H_{k-1}^{-1} * g_{k-1} \tag{2.7}$$

which is the gradient of the error rotated by multiplying with the Hessian of the loss function. Hence, for Newton's method all second order derivatives of the loss function have to be known analytically or estimated by finite difference techniques.

Gauss-Newton method assumes a small residual error in the loss function and thus approximates the Hessian as $J^T J$. Therefore, the Gauss-Newton Algorithm becomes,

$$\begin{aligned} \theta_k &= \theta_{k-1} - \eta_{k-1} * (J^T J)^{-1} * g_{k-1} \\ &= \theta_{k-1} - \eta_{k-1} * (J^T J)^{-1} * J_{k-1}^T f_{k-1} \end{aligned} \tag{2.8}$$

It approximately shares the properties of the general Newtons method but does not require a second order derivative to be calculated.

2.3 Decomposition of Interconnected System

This section provides an introduction to the generalized theory of diagonally dominant matrices and how diagonally dominant matrices can be used to reduce the complexity of an interconnected system.

2.3.1 Diagonally Dominant Matrices

Let A be any arbitrary square matrix with complex entries, which is partitioned in the following manner:

$$A = \begin{bmatrix} A_{1,1} & A_{1,2} & ... & A_{1,N} \\ A_{2,1} & A_{2,2} & ... & A_{2,N} \\ : & & & : \\ A_{N,1} & A_{N,2} & ... & A_{N,N} \end{bmatrix} \tag{2.9}$$

where, the diagonal submatrices $A_{i,i}$ are square of order n_i.

If the diagonal submatrices $A_{j,j}$ are non-singular and if

$$(||A_{j,j}^{-1}||)^{-1} \geq \sum_{k=1,k\neq j}^{N} ||A_{j,k}|| \qquad for\ all\ 1 \leq j \leq N \tag{2.10}$$

then A is block diagonally dominant relative to partitioning 2.9. We can define $(||A_{j,j}^{-1}||)^{-1}$ to be zero whenever $A_{j,j}$ is singular.

In the special case that all the submatrices $A_{i,j}$ are 1×1 matrices, then equation 2.10 becomes

$$|A_{j,j}| \geq \sum_{k=1,k\neq j}^{N} |A_{j,k}| \quad for\ all\ 1 \leq j \leq N \tag{2.11}$$

which is the general definition of diagonal dominance of a matrix [17] [13]. If strict inequality holds, then we say that the matrix is strictly diagonally dominant.

2.3.2 Dynamics of Interconnected Systems

We can write the conventional state space model of a large interconnected dynamical system as follows [31]:

$$\dot{x}_i = \tilde{A}_{ii}x_i + \sum_{j\neq i} \tilde{A}_{ij}x_j + \tilde{B}_i u_i \tag{2.12}$$

where $j \in C_i$ is set of connections to the subsystem i.

For network interconnected system, equation 2.12 can be re-written as

$$\dot{x}_i = A_{ii}x_i + \sum_{j\neq i} R_{ij}y_j + B_i u_i \tag{2.13}$$

where y_j are output variables measured at the interconnection of subsystem i and $j \in C_i$.

We need to first derive the conditions for decomposition of the interconnected system and then implement distributed parameter estimation for the model. Using the general Metzler conditions, we use the more restrictive but simpler diagonal dominance as sufficient conditions for decomposition [30] [18].

Using the definition given in equation 2.11, we can say that an uncontrolled interconnected dynamical system is diagonally dominant if the system matrix satisfies

$$|A_{ii,kk}| \geq \sum_{j \neq i} \sum_{r \neq k} |R_{ij,kr}| + \sum_{r \neq k} |A_{ii,kr}| \tag{2.14}$$

where $A_{ii,kk}$ is the k-th diagonal element of subsystem-i; $R_{ij,kr}$ is the r-th element of row-k of the interface between subsystem-i and subsystem-j; $A_{ii,kr}$ is the r-th element of row-k of subsystem-i.

Gershgorin Circle Theorem states that if a matrix is strictly diagonally dominant with all diagonal entries being negative, the real parts of its eigenvalues are also negative which suffices stability at equilibrium [17].

2.4 Energy-Power state space modelling

Conventional modelling of systems and control algorithms such as Automatic Generation Control (AGC) often suffer from a lack of scalability and cannot respond to fast persistent disturbances in the system . The system might also contain several smaller devices whose physical models are not always available. This problem has been a focus of our group who have been working on a novel aggregate modeling approach that utilizes energy/power space dynamics. This modelling approach addresses the fundamental issues of limited sensor measurements and still supports fast control implementation [22] [24]. This model relates the rate of change of work done and rate of change of work wasted because of the the interactions with the environment.

2.4.1 Pitfalls of Conventional Modelling

There has been extensive work and very detailed models designed for HVAC control, but upto our knowledge none of these controllers view an HVAC as a complex dynamical system whose efficiency can be enhanced by optimizing interactions between its different components. To do so, it is necessary to model different components to the degree of detail obtainable using available measurements [25].

The state of the art HVAC model used for ancillary services to the grid considers

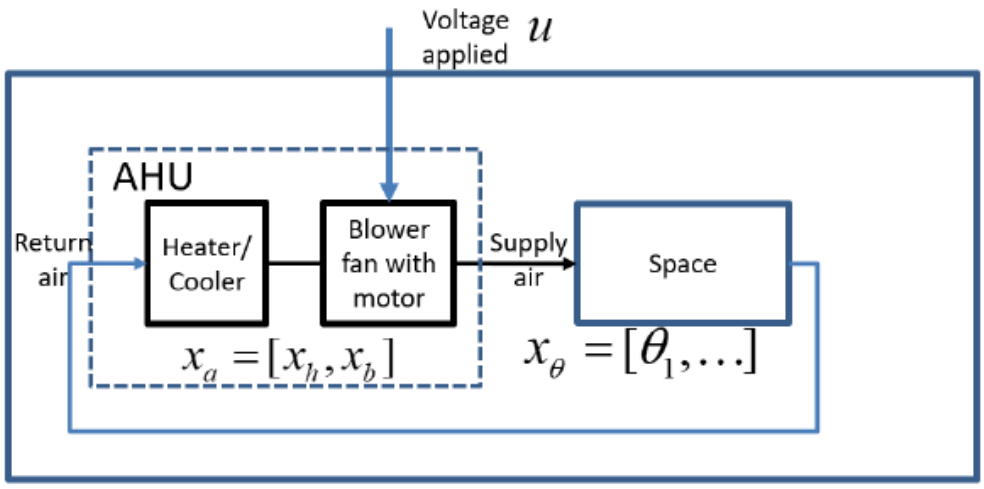

Figure 2-4: Schematic of a HVAC system in open loop (borrowed from [25])

an RC model of the thermal zone to be heated/cooled. We denote the state variables of the space using a vector x_T which represents the temperatures of various zones. These spaces are usually cooled using air blown from an Air Handling Unit or AHU. Let us denote the state variables of the AHU as x_a with states corresponding to the fan and motor in the AHU as x_f and x_m respectivly. Therefore, we can represent the dynamic model of the system as

$$\dot{x}_T = f_T(x_T, x_a) \tag{2.15}$$

$$\dot{x}_a = f_a(x_a, u) \tag{2.16}$$

An open-loop schematic for the same system is shown in Fig. 2-4. Here, depending on the choice of granularity required, the number of state variables in the model can grow extremely large. Also the exact models for the AHU and thermal zone are also complex [25]. Finally, obtaining the parameters of the model of the zone, f_T can be difficult making the model less accurate. We thus propose a simpler approach that uses aggregate energy variations in the next section.

2.4.2 Novel Energy-Power Modelling Methodology

The dynamical model of each component of a general system can be expressed in a standard state-space form as

$$\dot{x}_i = f'_{x,i}(x_i, u_i, m_i, r_i) \tag{2.17}$$

$$y_i = f'_{y,i}(x_i, u_i, m_i, r_i) \tag{2.18}$$

$$x_i(0) = x_{i,0} \tag{2.19}$$

where $x_i, u_i, m_i,\ r_i$ and y_i denote local states, inputs, local disturbances, port inputs and local outputs of interest respectively. A subset of the variables appear at the ports which can classified as either flow-type or effort-type. At the ports, one of these pairs is local to the component whereas the other is dictated by its connection to the rest of the system also called a port input.

It has been shown in [23], that using the state variable, and effort and flow variables at the port we can obtain the instantaneous real P_i and reactive power $\dot{Q}_i$ appearing at any of the ports as well as the stored energy E_i and stored energy in tangent space $E_{t,i}$.

We define a simple model that captures the dynamics of energy exchanges of a component with its neighbours by modelling the dynamics of aggregate variables, energy E and its rate of change as follows:

$$\dot{E} = P - \frac{E}{\tau} = p \tag{2.20}$$

$$\dot{p} = 4E_t - \dot{Q} \tag{2.21}$$

Here, the first equation denotes the first law of thermodynamics and states that the rate of change of stored energy is directly proportional to the power input minus the dissipative losses. The second equation corresponds to the second law of thermodynamics and highlights the inefficiencies in the system. This model was derived for general electrical circuits and was proven to hold for complex electro-mechanical systems with multi-energy conversions with the help of effort-flow analogy in different

domains [22] [25].

The dynamics of interaction variables $[E_i, p_i]$ captures the dynamics of internal energy conversion processes without the need to specify the type of energy conversion. Although, the variables $[E_i, p_i]$ are specific to a component, they are driven by the interactions from rest of the system through real and reactive power inputs.

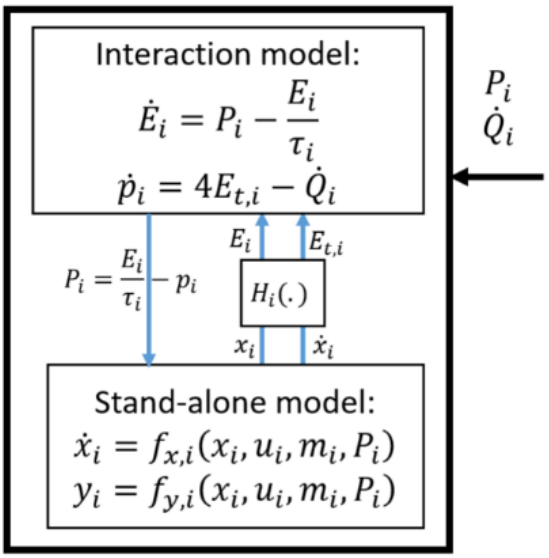

Figure 2-5: Stand-alone component in open-loop in energy space (borrowed from [23])

An example of a stand-alone component in open-loop in energy space can be seen in Fig. 2-5. The bottom layer with the detailed dynamics in conventional space is utilized for designing control in energy-power space and the top layer characterizes the input-output interactions of the component.

The model was originally derived for general electrical circuits and has proven to work for even complex electro-mechanical systems by extending the definitions of energy-power space variables using the effort-flow variable analogy in multi-energy domains.

2.4.3 HVAC Model in Energy-Power state space

The total stored energy of the HVAC system can be written as a sum of stored energy of the AHU (E_a) and the thermal energy of the zone (U) as follows:

$$\begin{aligned} E &= \int_{p_a(0)}^{p_a(t)} v_a^T dp_a + U \\ v_a &= [i_a, i_f, \omega_s] \end{aligned} \tag{2.22}$$

where, i_a, i_f and ω_s are the current through armature winding, current through armature field and angular velocity of shaft respectively [25].

For the total stored energy defined in 2.23, the first equation of the model in 2.21 can be used as

$$\dot{E} = -\frac{E}{\tau} + P_m \tag{2.23}$$

where, P_m is the input electrical power of the motor and τ being the overall time constant of the system dependant on system damping.

The generalized momentum variables can be expressed as a product of inertia matrix M_a and the generalized velocity variable v_a. The simplified expression for stored energy in tangent space can be written as

$$E_t = \frac{1}{2}\frac{dv_a^T}{dt} M_a \frac{dv_a}{dt} + \frac{1}{2} C_w \frac{dT^2}{dt} \tag{2.24}$$

where, C_w is the thermal constant of the zone. We can also write the total reactive power absorption by the AHU unit and the thermal zone as

$$\dot{Q}_a = F_a^T \frac{dv_a}{dt} - \frac{dF_a^T}{dt} v_a \tag{2.25}$$

$$\dot{Q}_T = T(\dot{S}_f^{in} + \dot{S}_f^{out}) - \dot{T}(S_f^{in} + S_f^{out}) \tag{2.26}$$

where, $\dot{S}_f^{in}$ and $\dot{S}_f^{out}$ are the entropy flow of the fluids at the inlet and outlet respectively. Similarly, we can define the controlled reactive power going into the

port of the motor as $\dot{Q}_m$.

Assuming a constant generalized inertia matrix, the second equation of general interaction model of a stand-alone component can be expressed as

$$\begin{aligned} \dot{p} &= 4E_t - (\dot{Q}_a - \dot{Q}_T) \\ &= 4E_T + 2\dot{Q}_T - \dot{Q}_m \end{aligned} \tag{2.27}$$

The term, $\dot{Q}_m$, essentially represents the inefficiencies in the system that are not related to damping losses. Thus the problem is translated into one where we want to maximize the efficiency by minimizing the cumulative instantaneous reactive power while satisfying the physical constraints of the system [25]. Therefore, the overall objective of the control can be posed as:

$$\min_{u(t)} \int_0^t \dot{Q_m}(s)^2 ds \tag{2.28}$$

Here, even though the underlying models in the conventional state space are unknown, the performance objective only depends on the unknown model through the terms E_t and Q_T which is of significance over much faster timescales [25] [22].

We can therefore utilize a two layered approach where the non-linear control design is performed locally to feedback linearized control in the energy-space.

Chapter 3

Approach

3.1 Overview

As mentioned before, designing control for a complex HVAC system such as the one shown in Fig. 2-3 can be extremely difficult due to several reasons mainly including the complexity and scalability of the model with the increasing number of components as well as the uncertainity in the conventional state space models that arise due to the unknown empirical parameters in the system.

Using measurement data from a real HVAC system, we will first try to obtain the parameters of some components of the HVAC system such as electric chiller and pump. Due to limited sensor measurements and the increased complexity due to more components, instead of estimating the parameters for the whole system at once, we try to develop a distributed algorithm for parameter estimation based on the diagonal decomposition property of positive systems.

We also analyze the modelling of these components in the energy-power space and use sensor data to verify that energy-space model agree with the conventional state models. In this verification process, we found that measurements from both effort and flow variables at the ports of a component are import for accurately calculating the rate of change of reactive power. The estimated parameters for the conventional models of these components can also be used for designing control in the energy-power space as mentioned in Section 2.4.2.

To completely understand the interconnected flow of energy and multi-energy conversions inside the HVAC system, we also analyze the energy consumption and its trends for several components. In the next few sections, we discuss the implementation and results obtained from the methodologies outlined in this section.

3.2 Energy Consumption inside the HVAC

The HVAC system show in Fig. 2-3 relies mainly on natural gas and electricity to meet its cooling/heating demands. The main consumers of electricity are the electric chillers, water pumps and cooling towers. The gas chillers and boilers use natural gas to produce chilled and heated water respectively. The internal combustion generators (ICGs) use natural gas to produce heat for warming the water and electricity to be used in the building or HVAC system.

3.2.1 Electricity consumption in HVAC

The electric chillers consume the most electricity inside the HVAC system. Each electric chiller is rated for a power consumption of 814 kW and a rated cooling capacity of 4571 kW. The electric chillers are only operational during the summers i.e. from May to September and is rarely used rest of the year. Most of the cooling needs during the rest of the months are met using the gas chillers. We can see the electricity consumption of both the electric chillers in Fig. 3-1.

The next biggest consumers of electricity in the HVAC system are the water pumps. We can see that there are currently 17 water pumps in the HVAC in Fig. 2-3. Out of the 17 pumps, only 7-8 pumps are operational at any given moment and the rest of the pumps are used as a backup. Most of the pumps in the system are rated for 75 kW of power consumption with a flow rate of 720 m^3/h. Some of the pumps are also rated for 37 kW of power consumption with a flow rate of 385 m^3/h but we rarely see them being operated. We can see the electricity consumption of two differnet pumps for the same time period in Fig. 3-2 (a) and (b). We can also see the total consumption of electricity per day for 7 days by all the pumps combined

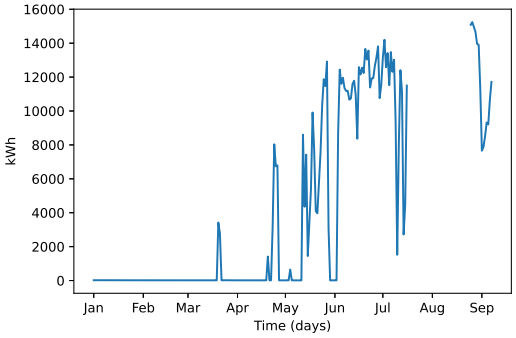

(a) Electric Chiller #1 (missing datapoints)

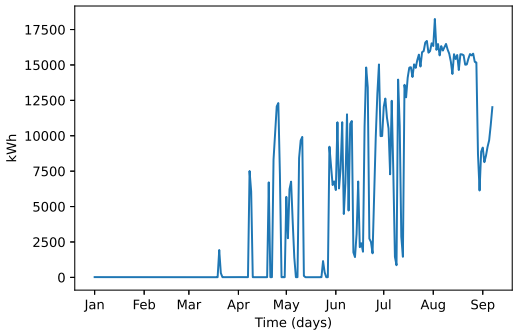

(b) Electric Chiller #2

Figure 3-1: Electricity consumption of Electric Chillers

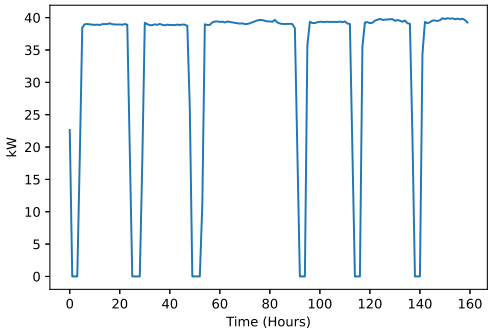

(a) 37 kW Pump

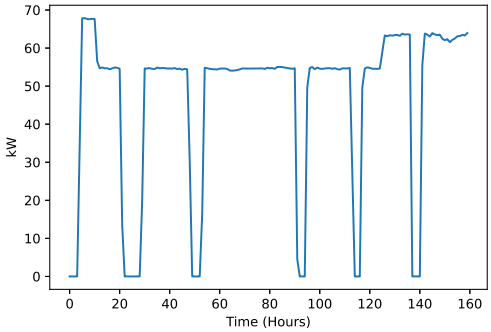

(b) 70 kW Pump

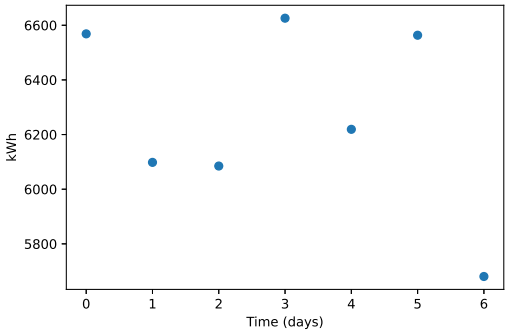

(c) Electricity consumed by all pumps

Figure 3-2: Electricity consumption of Water Pumps

in 3-2 (c).

We can see the total electricity consumed at the HVAC system in Fig. 3-3 (a).

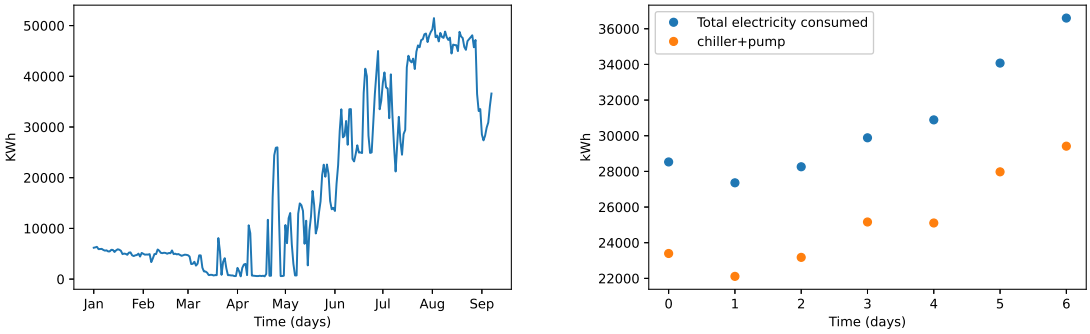

(a) Total Electricity Consumption of HVAC system

(b) Total vs Chiller and pump electricity consumption

Figure 3-3: Total Electricity Consumption of HVAC

This includes the energy consumed by electric chillers, water pumps and any other components needed to produce heating/cooling. We can also see the total electricity consumed and the electricity consumed by just electric chiller and water pumps for a few days in Fig. 3-3 (b). The electric chillers and water pumps make up 85% of the electricity consumed for production of heating/cooling. Due to lack of data, we are unable to exactly determine the consumers of the remaining 15% of electricity. We estimate that most of the remaining electricity is being consumed by the cooling towers shown in Fig. 2-3.

Thus, we have shown here that the electric chillers and the water pumps combined account for most of the electricity consumed in the HVAC system. In later sections, we show that these components use very rudimentary control strategies such as bang-bang control. Therefore, these two components will be the focus of the rest of the thesis and the aim will be to model these two components in the energy-power space so that more advanced control algorithms can be implemented to reduce the total electricity consumption.

3.2.2 Gas consumption in the HVAC

The consumers of natural gas in the HVAC system are the gas chillers, the internal combustion generators (ICG) and the water boiler. The ICG use the natural gas to

produce electricity for the HVAC and building, and the gas chiller and boiler cool/heat the water respectively.

The ICGs are rated for power production of 1160 kW and gas consumption of 317 Nm^3/h at the rated conditions. The ICGs are operated year round but they produce the most electricity during the peaks of winter and summer season when the most heating and cooling is required. We can see the production of electricity of each ICG daily in Fig. 3-4 (a) and (b). Fig. 3-4 (c) shows the total consumption of natural gas of both ICG combined.

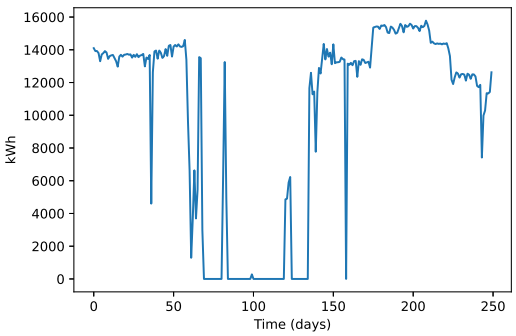

(a) ICG # 1

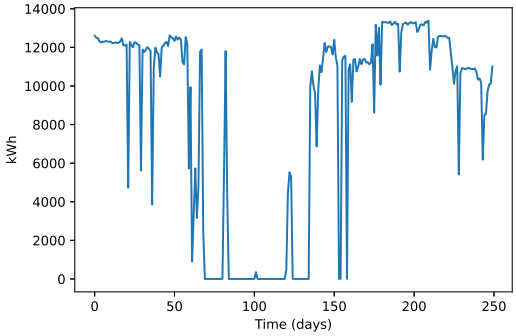

(b) ICG # 2

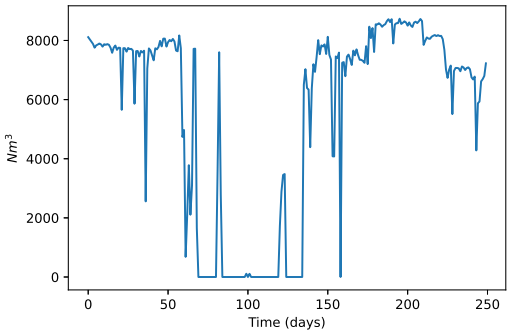

(c) Gas Consumption of both ICG

Figure 3-4: Gas consumption and electricity production of ICG

The consumption of natural gas by the boiler is shown in Fig. 3-5 (b). The boiler is rarely turned on because the heating demand of the building is low enough so that the waste heat from the ICGs can be used to heat up the water needed to meet the demand.

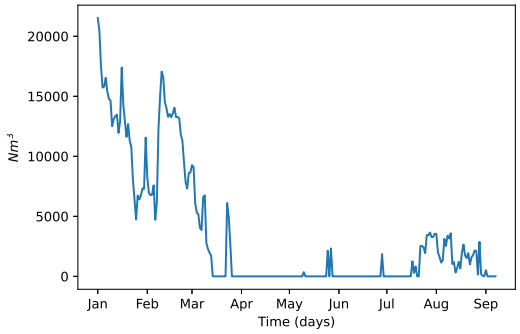

(a) Gas consumed by all gas chillers

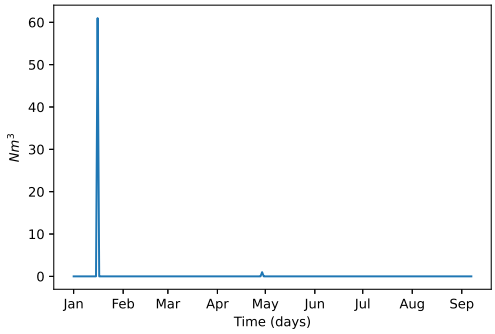

(b) Gas consumed by boiler

Figure 3-5: Gas consumption of Chiller and Boiler

The next biggest consumer of gas in the HVAC energy station are the gas chillers. The total gas consumption of all the gas chillers can be seen in Fig. 3-5 (a). The gas chillers are mostly operated during the winter season because the cooling demand is low and most of the cooling needs can be met using the gas chillers which are partially operated using the flue gases from the ICG thus reducing overall gas consumption. In contrast, as we see in Fig. 3-6 (b), the cooling demand in summer season is too high to be met by gas chillers alone and since electric chillers are more efficient, most cooling demand is met using electric chillers as can be seen in Fig. 3-1. That is why, the consumption of gas by gas chillers reduce during the months on June-September in Fig. 3-6 (a) despite the cooling demand being higher.

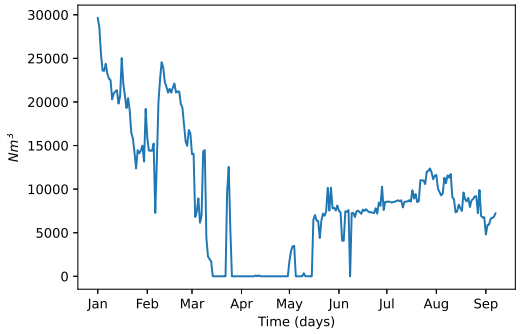

(a) Total gas consumption of HVAC

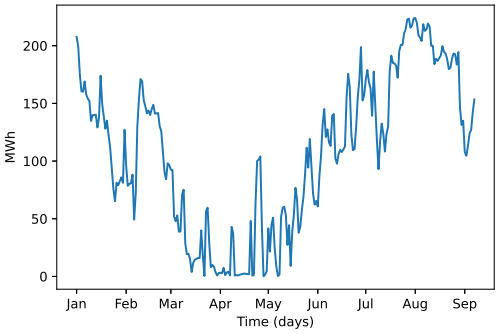

(b) Total cooling demand of the HVAC

Figure 3-6: Gas consumption and cooling demand of HVAC

3.3 Modelling of HVAC components in Conventional state space

In this section, without the loss of generality, we consider the conventional state space models of the water pump and the electric chiller. As we mentioned in the previous section, these two components are responsible for 85% of the electricity consumption of the entire HVAC. Thus, optimizing the control of these two components can result in huge increase in efficiency of HVAC. The gas chillers only supply a small portion of the cooling needs when the electric chillers are ON in the summer season. Due to the constraints on the data available, for the time being we ignore the gas chillers in our modelling efforts.

3.3.1 Electric Chiller Model

The chiller model describes the energy balance between the chiller energy input, the thermal energy stored in the tank, the heat gain through return water from the coils and from the environment. We assume the simplification that the internal variables and control of the chiller work properly and stabilize the subsystem quickly [34] [35]. Therefore, we only consider the slower water temperature dynamics in our model.

The electric chiller is a complex dynamical subsystem but with the above assumption, we can model it using a reduced first-order Coefficient of Performance (COP) equation as:

$$\frac{d}{dt}T_{ws} = \frac{1}{\rho_w c_w V_{tank}}(-\dot{m}_w c_w (T_{ws} - T_{wr}) - U_c E_c COP + \alpha_h (T_{\infty,t} - T_{ws})) \qquad (3.1)$$

where, T_{ws} is the state of the chiller and denotes the temperature of the chilled water supplied to the coils, T_{wr} is the temperature of the water returned from coils and $T_{\infty,t}$ is the sink temperature or temperature of water used to cool the chiller [38] [34].

We can also represent equation 3.1 using the lumped-parameter equation as follows

$$\frac{d}{dt}T_{ws} = -\alpha_1\big(T_{ws} - T_{wr}\big) - \alpha_2 U_c - \alpha_3 T_{ws} + \alpha_4 \tag{3.2}$$

where, the lumped parameters are given by

$$\begin{aligned} \alpha_1 &= \frac{1}{\rho_w V_{tank}} \\ \alpha_2 &= \frac{E_c COP}{\rho_w c_w V_{tank}} \\ \alpha_3 &= \alpha_h \\ \alpha_4 &= T_{\infty,t} * \alpha_h \\ \alpha_1, \alpha_2, \alpha_3, \alpha_4 &> 0 \end{aligned}$$

α_1 is the coefficient that relates the mass flow of the supply water and the temperature difference between supply and return water to the change in supply water temperature. α_2 links the input power or control of the chiller to the supply water temperature. α_3 is the damping coefficient of the supply temperature and α_4 depends on the environment temperature.

3.3.2 Water Pump Model

The chilled water in the HVAC is pumped from the chiller to the cooling and dehumidifying coils through a single loop. Therefore, the state space model of the piping system connected to the pumps can represented with the following equation:

$$\frac{d\dot{m}_w}{dt} = \Delta P_p - \Delta P_v - f_{p,1} - f_{p,2} - \Delta P_{t,in} - \Delta P_{t,out} \tag{3.3}$$

where ΔP_p is the pressure increase from the pump, ΔP_v is the pressure drop over a valve, $f_{p,i}$ is the pressure drop due to friction in the pipe, and $\Delta P_{t,in}$ and $\Delta P_{t,out}$ are the pressure drops corresponding to expansion and extraction respectively [38].

We can also write these terms as follows:

$$f_{p,i} = \frac{C_f A_d L_{p,i}}{2\rho_w A_i^3}\dot{m}_w^2 \tag{3.4}$$

$$\Delta P_p = C_h \rho_w D^2 (\frac{n_m}{n_p})^2 N_p^2 \tag{3.5}$$

$$\Delta P_{t,in} = \frac{\xi_{in}}{2\rho_w A_{in}^2}\dot{m}_w^2 \tag{3.6}$$

$$\Delta P_{t,out} = \frac{\xi_{out}}{2\rho_w A_{out}^2}\dot{m}_w^2 \tag{3.7}$$

$$\Delta P_v = \frac{\alpha_1 U_v^{\alpha_2}}{2\rho_w A^2}\dot{m}_w^2 \tag{3.8}$$

The pump-motor model can be written as,

$$\frac{d}{dt}N_p = \frac{k_i}{2\pi J_p}I_p - \frac{B_p}{J_p}N_p - h_{13}\dot{m}_w N_p \tag{3.9}$$

$$\frac{d}{dt}I_p = -\frac{R_{a,p}}{L_{a,p}}I_p - \frac{2\pi k_{b,p}}{L_{a,p}}N_p + \frac{e_{a,p}}{L_{a,p}}U_p \tag{3.10}$$

where, N_p is the pump rotational frequency; I_p is the armature current of pump motor; is the water mass flow rate; U_p is the voltage applied to the terminals of armature as a control signal [38].

The lumped-parameter equation of the complete water pump model can be represented as

$$\frac{d}{dt}N_p = h_{11}I_p - h_{12}N_p - h_{13}\dot{m}_w N_p \tag{3.11}$$

$$\frac{d}{dt}I_p = -h_{21}I_p - h_{22}N_p + h_{23}U_p \tag{3.12}$$

$$\frac{d}{dt}\dot{m}_w = \frac{1}{2}(h_{31}N_p^2 - h_{32}\dot{m}_w^2) \tag{3.13}$$

where the lumped parameters are given by

$$h_{11} = \frac{k_i}{2\pi J_p} \tag{3.14}$$

$$h_{12} = \frac{B_p}{J_p} \tag{3.15}$$

$$h_{13} = h_{13} \tag{3.16}$$

$$h_{21} = \frac{R_{a,p}}{L_{a,p}} \tag{3.17}$$

$$h_{22} = \frac{2\pi k_{b,p}}{L_{a,p}} \tag{3.18}$$

$$h_{23} = \frac{e_{a,p}}{L_{a,p}} \tag{3.19}$$

$$h_{31} = C_h \rho_w D^2 (\frac{n_m}{n_p})^2 \tag{3.20}$$

$$h_{32} = \frac{C_f A_d}{2\rho_w} \frac{L_{p1}}{A_1^3} + \frac{C_f A_d}{2\rho_w} \frac{L_{p2}}{A_2^3} + \frac{\xi_{in}}{2\rho_w A_{in}^2} + \frac{\xi_{out}}{2\rho_w A_{out}^2} + \frac{\alpha_1 U_v^{\alpha_2}}{2\rho_w A^2} \tag{3.21}$$

$$h_{11}, h_{12}, h_{13}, h_{21}, h_{22}, h_{23}, h_{31}, h_{32} > 0$$

$h_1 3$ relates the torque of the pump to the water mass flow. $h_3 1$ is the coefficient that relates the pressure head difference to the current of the water pump and $h_3 2$ aggregates all the friction and pressure drop terms of the pump.

Combining the equations 3.13, 3.11 and 3.12, we obtain a third order model of the water pump, given by,

$$\frac{dx_w}{dt} = \begin{bmatrix} f_1(\dot{m}_w, N_p, U_v) \\ f_2(\dot{m}_w, N_p, I_p) \\ f_3(N_p, I_p, U_p) \end{bmatrix} \tag{3.22}$$

$$x_w = [\dot{m}_w \ N_p \ I_p]^T \tag{3.23}$$

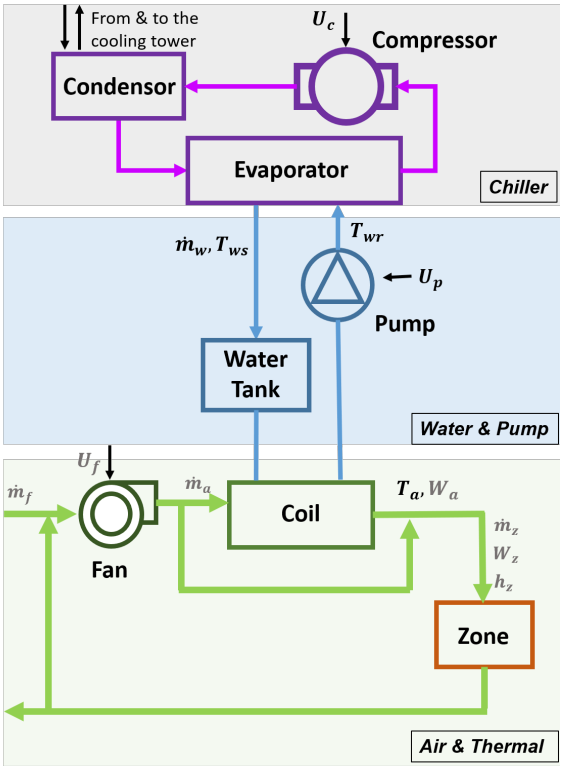

Figure 3-7: Interaction of pump and chiller subsystem with the HVAC [33]

3.3.3 Chiller and Pump combined model

There are 8 pumps that supply water for cooling/heating to all the chillers and boiler as shown in Fig. 2-3. For the time period under consideration, only 3 out of the 8 pumps are operational. All the pumps are identical and use the same control logic for operating. Therefore, moving forward in our analysis, we will model the three pumps combined as a single pump and the parameters of the new model will be the equivalent parameters of the 3 pumps.

Therefore, the we can write the model equation for the chiller and water pump subsystem by combining equations 3.1 and 3.22 as given:

$$\frac{dx_w}{dt} = \begin{bmatrix} f_1(\dot{m}_w, N_p, U_v) \\ f_2(\dot{m}_w, N_p, I_p) \\ f_3(N_p, I_p, U_p) \\ f_4(\dot{m}_w, T_{ws}, T_{wr}, U_c) \end{bmatrix} \tag{3.24}$$

$$x_w = [\dot{m}_w \ N_p \ I_p \ T_{ws}]^T \tag{3.25}$$

We can also see in Fig. 3-7 , how this subsystem composed the of chiller and water pumps interact with the rest of the HVAC system. The subsystem also interacts with the coils and the environment. We assume that the heat exchange between the water and the air in the coil is very fast and thus can be treated as instantaneous states. Also since the temperature response of the environment is much slower, we treat its variables as constants.

3.4 Decoupling of Chiller and Pump subsystem

For the illustration of our approach, we analyse the conditions under which a distributed parameter estimation approach can yield results that are as accurate as modelling and estimating the parameters of the chiller-pump combined subsystem. We use the methodology that when two systems are weakly coupled, each subsystem can only exert limited influence on the other subsystem through the interface variables. Therefore, a distributed parameter approach can be used for such subsystems.

3.4.1 Assumptions

Let's consider the linearized approximation of equation 3.24 [33],

$$\frac{d}{dt}\begin{bmatrix} \delta N_p \\ \delta I_p \\ \delta \dot{m}_w \\ \delta T_{ws} \end{bmatrix} = \begin{bmatrix} A_{11} & A_{12} \\ A_{21} & A_{22} \end{bmatrix} \begin{bmatrix} \delta N_p \\ \delta I_p \\ \delta \dot{m}_w \\ \delta T_{ws} \end{bmatrix} \tag{3.26}$$

where the submatrices are given by

$$A_{11} = \begin{bmatrix} -(h_{12} + h_{13}\dot{m}_w) & h_{11} \\ -h_{22} & -h_{21} \end{bmatrix} \tag{3.27}$$

$$A_{12} = \begin{bmatrix} -h_{13}N_p & 0 \\ h_{23}\frac{\partial U_p}{\partial \dot{m}_w} & h_{23}\frac{\partial U_p}{\partial T_{ws}} \end{bmatrix} \tag{3.28}$$

$$A_{21} = \begin{bmatrix} h_{31}N_p & 0 \\ 0 & 0 \end{bmatrix} \tag{3.29}$$

$$A_{22} = \begin{bmatrix} -h_{33}\dot{m}_w & 0 \\ \alpha_1(T_{wr} - T_{ws}) & -\alpha_1\dot{m}_w - \alpha_3 - \frac{\partial(\alpha_2 U_c)}{\partial T_{ws}} \end{bmatrix} \tag{3.30}$$

Assumption 1: *The chiller subsystem can be modeled using the reduced first-order equation 3.2*

In Section 3.3.1, we take use the reduced order model of the chiller and assume that the control stabilizes the chiller quickly. At the quasi steady state the supplied water temperature T_{ws} should be close to a reference temperature T_{ref} set by the system operator. Therefore, based on the first-order model in equation 3.2, the control of the chiller U_c should be proportional to the temperature difference $T_{wr} - T_{ws}$. We can see the relationship between the measurement data for control U_c and temperature difference $T_{wr} - T_{ws}$ in Fig. 3-8. From that figure, we can verify the assumption 1 that the chiller can be modelled using the reduced dynamical equation.

Assumption 2: *The natural responses of the states I_p and N_p of the pump are much faster than the natural response of other internal state, water mass flow $\dot{m}_w$.*

This assumption will be verified later in Section 5, when we find the parameters

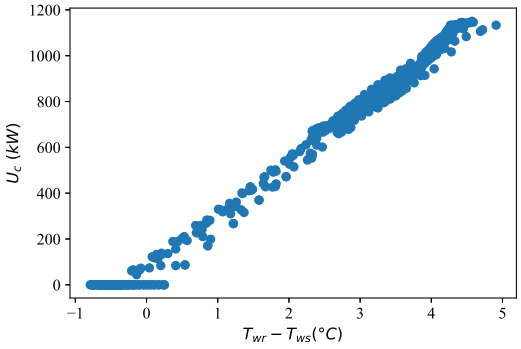

Figure 3-8: Chiller control vs Temperature difference across chiller [33]

for the water pump model.

Using Assumption 2, we can set the differential of N_p and I_p to 0 in equation 3.26 [33],

$$\begin{aligned} \frac{d}{dt}\begin{bmatrix} 0 \\ 0 \\ \delta\dot{m}_w \\ \delta T_{ws} \end{bmatrix} &= \begin{bmatrix} A_{11} & A_{12} \\ A_{21} & A_{22} \end{bmatrix} \begin{bmatrix} \delta N_p \\ \delta I_p \\ \delta\dot{m}_w \\ \delta T_{ws} \end{bmatrix} \\ \implies A_{11}\begin{bmatrix} \delta N_p \\ \delta I_p \end{bmatrix} &= A_{12}\begin{bmatrix} \delta\dot{m}_w \\ \delta T_{ws} \end{bmatrix} \\ \frac{d}{dt}\begin{bmatrix} \delta\dot{m}_w \\ \delta T_{ws} \end{bmatrix} &= A_{21}\begin{bmatrix} \delta N_p \\ \delta I_p \end{bmatrix} + A_{22}\begin{bmatrix} \delta\dot{m}_w \\ \delta T_{ws} \end{bmatrix} \end{aligned} \tag{3.31}$$

Then, equation 3.31 can be simplified to

$$\frac{d}{dt}\begin{bmatrix} \delta\dot{m}_w \\ \delta T_{ws} \end{bmatrix} = \left[A_{22} - A_{21}A_{11}^{-1}A_{12}\right]\begin{bmatrix} \delta\dot{m}_w \\ \delta T_{ws} \end{bmatrix} \tag{3.32}$$

Assumption 3: *The control signal for the pump, U_p, for the pump is bang-bang control type which only takes values as ON and OFF.*

We use sensor measurements of the pump armature current in Fig. 3-9. From the

figure, we can infer that the current I_p is a step response for the given precision and changes in response to the supply water temperature T_{ws}. Therefore, it verifies our third assumption.

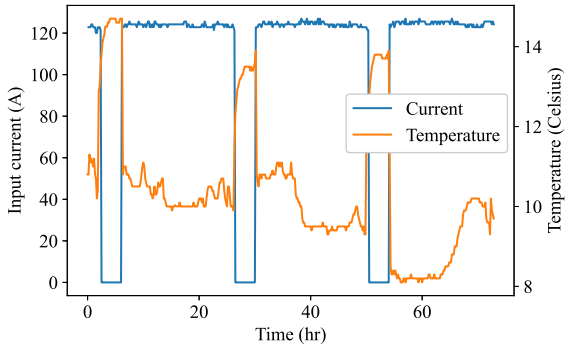

Figure 3-9: Pump control in response to supplied water temperature [33]

Hence, $\frac{\partial U_p}{\partial}$ and $\frac{\partial U_p}{\partial T_{ws}}$ can be set to zero almost everywhere. So, the submatrix $A_{21}A_{11}^{-1}A_{12}$ in equation 3.32 becomes [33],

$$\begin{aligned} A_{21}A_{11}^{-1}A_{12} &= \begin{bmatrix} h_{32}N_p & 0 \\ 0 & 0 \end{bmatrix} \begin{bmatrix} -(h_{12}+h_{13}\dot{m}_w) & h_{11} \\ -h_{22} & -h_{21} \end{bmatrix}^{-1} \begin{bmatrix} -h_{13}N_p & 0 \\ 0 & 0 \end{bmatrix} \\ &= \begin{bmatrix} d_{11} & 0 \\ 0 & 0 \end{bmatrix} \end{aligned} \tag{3.33}$$

where

$$d_{11} = \frac{h_{13}h_{31}}{h_{11}h_{22} - h_{13}\dot{m}_w + h_{12}} N_p^2 \tag{3.34}$$

Therefore, the Jacobian matrix in equation 3.32 can be written as

$$\frac{d}{dt}\begin{bmatrix} \delta\dot{m}_w \\ \delta T_{ws} \end{bmatrix} = \begin{bmatrix} -h_{33} - d_{11} & 0 \\ \alpha_1(T_{wr} - T_{ws}) & -\alpha_1\dot{m}_w - \alpha_3 - \frac{\partial(\alpha_2 U_c)}{\partial T_{ws}} \end{bmatrix} \begin{bmatrix} \delta\dot{m}_w \\ \delta T_{ws} \end{bmatrix} \tag{3.35}$$

3.4.2 Coupling between Pump and Chiller

The first row of the Jacobian in 3.35 only has the first entry non-zero, therefore, $\frac{d}{dt}\dot{m}_w$ is diagonal dominant.

From parameter estimation in Section 5 and rated values of the chiller we obtain that $\alpha_1 = 0.0660$, α_3 - 5.0427, $\dot{m}_w = 170$ kg/s, $T_{ws} = 7$ and $T_{wr} = 13$. Note that $\frac{\partial \alpha_2}{\partial T_{ws}} = \frac{COP_{max}-1}{\Delta T_{max}} E_c > 0$ [33].

Thus substituting these values in equation 3.35, we get,

$$\begin{bmatrix} -h_{33} - d_{11} & 0 \\ 0.396 & -16.24 - \frac{\partial(\alpha_2 U_c)}{\partial T_{ws}} \end{bmatrix} \tag{3.36}$$

Using the conditions for diagonal dominance mentioned in Section 2.3, we can conclude that T_{ws} is also diagonal dominant. Therefore, the coupling between the states of the chiller and pump i.e. T_{ws} and $\dot{m}_w$ is weak and the distributed parameter estimation can achieve good performance under the given assumptions. We further verify our methodology by validating the simulation data obtained from estimated parameters in Section 5 [33].

Assumption 3 greatly simplifies our approach because if it is not valid and more sophisticated control strategies are used for the water pump, then $\frac{\partial U_p}{\partial \dot{m}_w}$ and $\frac{\partial U_p}{\partial T_{ws}}$ may not vanish everywhere. For example, lets assume the pump uses proportional gain control,

$$U_p = \begin{cases} K_p(T_{ws} - T_{ref}) & \text{if } T_{ws} > T_{ref} \\ 0 & \text{else.} \end{cases} \tag{3.37}$$

where T_{ref} is the reference temperature of the supply water set by a system operator. Thus,

$$\frac{\partial U_p}{\partial \dot{m}_w} = \frac{\partial U_p}{\partial T_{ws}} \frac{\partial T_{ws}}{\partial \dot{m}_w} = \begin{cases} K_p \frac{\partial T_{ws}}{\partial \dot{m}_w} & \text{if } T_{ws} > T_{ref} \\ 0 & \text{else} \end{cases} \tag{3.38}$$

$$\frac{\partial U_p}{\partial T_{ws}} = \begin{cases} K_p & \text{if } T_{ws} > T_{ref} \\ 0 & \text{else} \end{cases} \tag{3.39}$$

Hence, we get,

$$A_{21} A_{11}^{-1} A_{12} = \begin{bmatrix} \tilde{d}_{11} & \tilde{d}_{12} \\ 0 & 0 \end{bmatrix} \tag{3.40}$$

where,

$$\tilde{d}_{11} = d_{11} - \frac{e_{a,p} h_{31} k_i N_p K_p}{2\pi (k_i k_{b,p} - h_{13} R_{a,p} J_p \dot{m}_w + B_p R_{a,p})} \frac{\partial T_{ws}}{\partial \dot{m}_w} \tag{3.41}$$

$$\tilde{d}_{12} = -\frac{e_{a,p} h_{31} k_i N_p K_p}{2\pi (k_i k_{b,p} - h_{13} R_{a,p} J_p \dot{m}_w + B_p R_{a,p})} \tag{3.42}$$

Therefore, the Jacobian matrix in 3.32 becomes,

$$\begin{bmatrix} -h_{33} - \tilde{d}_{11} & -\tilde{d}_{12} \\ \alpha_1 (T_{wr} - T_{ws}) & -\alpha_1 - \alpha_3 - \frac{\partial (\alpha_2 U_c)}{\partial T_{ws}} \end{bmatrix} \tag{3.43}$$

Since, increasing the control gain K_p decreases the value of $\tilde{d}_{11}$ and thus, increases the value of the first term of firt row of 3.43. Therefore, a large value of control gain K_p can destabilize the coupled system. In this case, $\dot{m}_w$ is strongly coupled with T_{ws} and the distributed parameter estimation will be less accurate than before [33].

3.5 Distributed Parameter Estimation

The section represents an approach to identify critical parameters of the chiller and pump model in a distributed manner assuming a weakly coupled system. We use the estimation method mentioned in Section 2.2 for chiller and pump individually. This greatly reduces the computational complexity and the amount of data needed for estimation.

We can rewrite the chiller model in equation 3.2 in the form of equation 2.13 as follows [33]:

$$\frac{d}{dt}T_{ws} = A_{ii}T_{ws} + \sum_{j\neq i} R_{ij}[\dot{m}_w \; T_{wr}]^T + B_i u_i + \alpha_4 \tag{3.44}$$

where,

$$\begin{aligned} A_{ii} &= -\alpha_1 - \alpha_3 \\ \sum_{j\neq i} R_{ij} &= \tfrac{1}{2}\alpha_1[T_{wr} \; \dot{m}_w] \\ B_i &= -\alpha_2 \\ u_i &= U_c \end{aligned}$$

Since, the pump and chiller are weakly coupled, we can treat m_w as another interface variable. Therefore, we can group it with other interface variables and use sensor measurements instead of calculating it dynamically.

Using the estimated parameters, the output of the augmented chiller equation in (3.2) i.e. $\hat{T}_{ws,i}$ is compared with experimental data i.e. $T_{ws,i}$. The error is given by

$$Error = \sum_{k=0}^{n}(T_{ws,k} - \hat{T}_{ws,k})^2 = \sum_{i=0}^{n} f(k) \tag{3.45}$$

Similarly, using equation 2.8, we can write the parameter update equation for

chiller as:

$$\alpha_k = \alpha_{k-1} - \eta_{k-1} * (J^T J)^{-1} * g_{k-1} \tag{3.46}$$
$$\alpha_k = [\alpha_{1,k}\ \alpha_{2,k}\ \alpha_{3,k}\ \alpha_{4,k}]^T$$

Similarly, we can write the parameter update and error equations for pump and other components in the HVAC system.

3.6 Energy Space model for chiller

To design the energy space model for the electric chiller, first we need to understand the interaction of variables P and $\dot{Q}$ for different components of the HVAC. We can see these interactions for the water flow subsystem and the electric chiller in Fig. 3-10 [14].

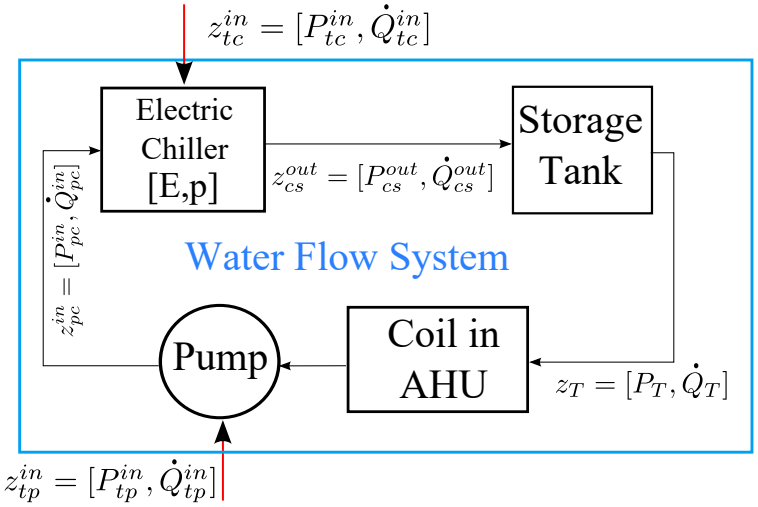

Figure 3-10: Interface varibales for the HVAC system [14]

We also need to understand the interactions of the chiller in the conventional state space to accurately map the system from conventional state space to energy space. The interactions of the chiller in conventional state space can be seen in Fig. 3-11 (a) and the corresponding interactions using the variables P and $\dot{Q}$ can be seen in 3-11 (b).

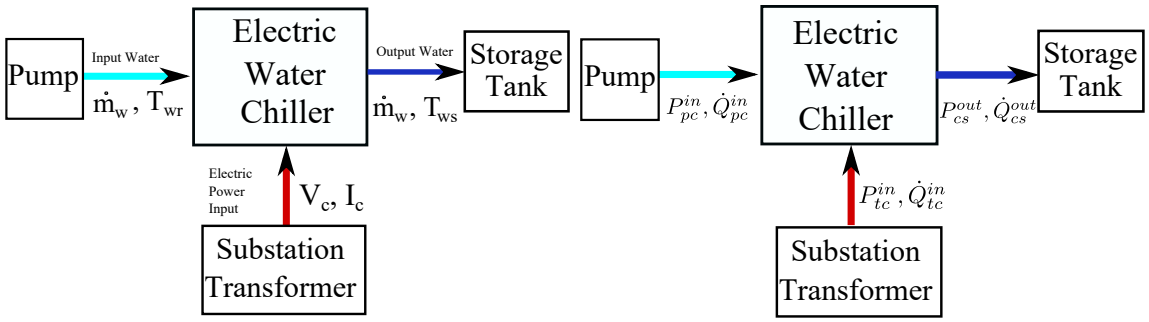

(a) Conventional state space model of chiller (b) Energy power space model of chiller

Figure 3-11: Chiller models in conventional and energy state space[1][14]

Energy domain	Effort variable (e)	Flow variable (f)	Real power (P)	Reactive power rate ($\dot{Q}$)
Electric	Voltage (v)	Current (i)	vi	$vi - iv$
Translation	Force (F)	Velocity (u)	Fu	$Fu - uF$
Rotational	Torque (τ)	Angular velocity (ω)	$\tau\omega$	$\tau\omega - \omega\tau$
Fluid	Pressure (Pr)	Volume flow (f)	$Pr\ f$	$Prf - fPr$
Thermodynamic	Temperature (T)	Entropy flow (S)	TS	$TS - ST$

Table 3.1: Analogous effort and flow variables across different energy domains [24]

The water entering the chiller has two components i.e. the thermal component corresponding to the temperature of the water and the fluid component corresponding to the pressure of the water. The thermal component is characterized by the temperature (terminal effort) and entropy flow rate (flow variable), which are together used to define the generalized real power and the generalized reactive power rate in thermal domain. The fluid component is characterized by the pressure (effort variable) and volume flow rate (flow variable) in fluid domain, as reflected from Table 3.1.

Using the thermal and fluid components of incoming and outgoing water, and using the input electrical power, the equations for generalized power P and generalized rate of reactive power $\dot{Q}$ as shown in Section 2.4.2 can be written as [14]

$$P_{pc}^{in} = c_w \dot{m}_w T_{wr} + (1/\rho_w)\dot{m}_w Pr_{ci} \tag{3.47}$$

$$P_{cs}^{out} = c_w \dot{m}_w T_{ws} + (1/\rho_w)\dot{m}_w Pr_{co} \tag{3.48}$$

$$P_{tc}^{in} = I_c V_c \tag{3.49}$$

[1]In joint collaboration with Marija Ilic and Pallavi Bharadwaj

$$\dot{Q}^{in}_{pc} = c_w(\dot{m}_w T_{wr} - \dot{m}_w T_{wr}) + (1/\rho_w)(Pr_{ci}\dot{m}_w - \dot{m}_w Pr_{ci}) \quad (3.50)$$

$$\dot{Q}^{out}_{cs} = c_w(\dot{m}_w T_{ws} - \dot{m}_w T_{ws}) + (1/\rho_w)(Pr_{co}\dot{m}_w - \dot{m}_w Pr_{co}) \quad (3.51)$$

$$\dot{Q}^{in}_{tc} = V_c I_c T_{wr} - I_c V_c \quad (3.52)$$

where, Pr_{ci} and Pr_{co} are the input and output pressure in the chiller respectively.

Therefore, the total power P and total rate of reactive power $\dot{Q}$ into the chiller can be written as

$$P = P^{in}_{pc} + P^{in}_{tc} - P^{out}_{cs} \quad (3.53)$$

$$\dot{Q} = \dot{Q}^{in}_{pc} + \dot{Q}^{in}_{tc} - \dot{Q}^{out}_{cs} \quad (3.54)$$

This methodology can be generalized to other components of the HVAC. Usually, a commercial HVAC system measures temperature, pressure and mass flow of water and air at regular intervals which can be used to calculate the power and reactive power at the interface for different subsystems.

Chapter 4

Implementation

This section presents the underlying details of the implementation of the approach for parameter estimation and energy power space modelling mentioned in Section 3.

4.1 Data Description

We obtained data regarding various sensor measurements regarding a commercial HVAC system shown in Fig. 2-3. The complete list of data obtained can be seen in Table. 4.1. We have the chiller and pump data for 7 days sampled every 10 minutes. We also have the data available regarding the energy consumption of different components of the HVAC sampled once daily from January to September. The daily sampled data denotes the cumulative energy consumption for that day.

System	Symbol	Description	Sampling Time
Pump	$\dot{m}_w$	Water flow rate	10 minutes
	N_p	Pump speed/frequency	10 minutes
	I_p	Pump current	10 minutes
Chiller	T_{wr}	Return water temperature	10 minutes
	T_{ws}	Supply water temperature	10 minutes
	U_c	Chiller control input	10 minutes
HVAC		Gas consumption of HVAC	24 hours
		Electricity consumption of HVAC	24 hours
		Water consumption of HVAC	24 hours
		Electricity generated by each ICG	24 hours
		Gas consumption of gas chillers	24 hours
		Gas consumption of boiler	24 hours
		Electricity consumption of each ECR	24 hours

Table 4.1: Summary of measurement data from the HVAC

4.2 System Identification in MATLAB

We use MATLAB's system identification toolbox to estimate critical parameters in differential equations. We use several functionalities within the non-linear grey-box model estimation module to implement the approach mentioned in Section 3 [8] [1].

First, we need to create a model file for the subsystem whose parameters we need to identify. We can see an example of a model file in Fig. 4-1 for chiller subsystem represented by equation 3.2.

```
function [dx, y] = chiller_model2(t,x,u,a1,a2,a3,a4,FileArgument)
%Define the model using inputs and state variables

Uc = u(1); %chiller control
mw = u(2); %water flow rate
Twr = u(3);%return water temperature

%Define the state variable dynamics
dx = x*(-a1*mw-a3) - a2*Uc + a4 + a1*mw*Twr ;
%Set output equal to state variable
y = x;

end
```

Figure 4-1: Chiller MATLAB Model file

Once, we have defined the system model using a model file, we can use *idnlgrey* function in the system identification toolbox to create a non-linear grey box model of the given model file [2]. An example for the chiller model file is shown in Fig. 4-2. We need to specify the model file using filename parameter, the order of inputs and outputs to the model, the initial guess of the parameter values, an initial value for the state variable and time units for the model.

Once we have completed specifying the initial conditions for the model, we can use an optimizer to learn the model using measurement data. To build and run an optimizer we need two functions from the MATLAB toolbox i.e. *nlgreyest* for estimating non-linear grey box models and *nlgreyestOptions* for specifying the optimization parameters and conditions [3] [4]. An example of how this can be used for the chiller

```
%specify model file name
filename = 'chiller_model_with_control';
order = [1 3 1]; %[state variables, inputs, ouputs]
Parameters = [0.0066;0.0000202;0.50089;21]; %initial parameters
initial_state = [x0]; %initial state
Ts = 0; %continuous time model

%create grey box model
nlgr = idnlgrey(filename, order, Parameters, initial_state, Ts);
nlgr.TimeUnit = 'seconds'; %specify time units
```

Figure 4-2: Chiller grey box model in MATLAB

subsystem is shown in Fig. 4-3

```
%specify optimizer options
opt = nlgreyestOptions('Display', 'on');
opt.SearchOptions.MaxIterations = 50;
opt.SearchOptions.FunctionTolerance = 1e-7;

%estimate the grey box model parameters
nlgr = nlgreyest(z, nlgr, opt)
```

Figure 4-3: Chiller grey box model optimization in MATLAB

Using the *nlgreyestOptions* functionality, we can try different optimizers, ODE solvers, function tolerances etc. to tune our optimizer to our needs. We have found that for a single ODE system such as chiller, the default parameters of the optimizer work well and run in sufficient time. But for more complex systems such as the water pump with multiple ODE's changing the parameters of the optimizer can help reduce the computational time by a lot.

Once we execute this code, the grey box model outputs the parameters which result in the least error given by 3.45.

4.3 Energy space model verification in Python

We use Python to prepare the data regarding the input and output interface variables of the chiller and to verify the chiller energy-space model. We use Python packages such as *Numpy*, *Pandas* and *Statistics* to manage the data and then use it to verify the fundamental equations given by equation 2.21 [5] [6] [7].

We use the *Pandas* module to import and cleanse the data. An example can be seen in Fig. 4-4. In the figure, the *Pandas* module is abbreviated as pd.

```
#Read the csv file
df = pd.read_csv("../../data/chiller_final_data.csv")

#Drop the unnecessary columns
df = df.drop(columns = ['time_T','time_xls_power','date',
                        'x2_ElectricAirConditionerPowerConsumption_KWh',
                        'time_T2','time_xls_current'])

#Rename columns for better understanding
df.columns = ['time','Twr','Tws','water','power','current']
```

Figure 4-4: Importing data using Python

We then use the *Numpy* module to do basic arithmetic operations on the imported data so that we can then further use that data for advanced mathematical operations such as integration and differentiation. We can see us using *Numpy* module for changing units of imported data in Fig. 4-5.

```
#Converting data to SI units
e_elec = df.power.to_numpy()*1000.0*3600.0 #Ws
p_elec = df.power.to_numpy()*6000.0 #W
tws = df.Tws.to_numpy() +273.15  #K
mw = df.water.to_numpy()*1000.0/3600.0 #kg/s
twr = df.Twr.to_numpy() +273.15  #K
i = df.current.to_numpy() #Ampere
```

Figure 4-5: Using Numpy to convert units of data

We can also see another example of *Numpy* being used to calculate the rate of reactive power flow across the chiller in Fig. 4-6. Here, we use *Numpy* module's ability to do arithmetic operations on arrays.

```
#calculate rate of thermal reactive energy input
dqin = cw*(np.multiply(twr,dmw) - np.multiply(dtwr,mw)) +
        (np.multiply(pr_in,dmw) - np.multiply(mw,dpr_in))/rw

#calculate rate of thermal reactive energy output
dqout = cw*(np.multiply(tws,dmw) - np.multiply(dtws,mw)) +
        (np.multiply(pr_out,dmw) - np.multiply(mw,dpr_out))/rw

#calculate rate of electrical reactive energy input
dq_elec = np.multiply(di,v) - np.multiply(dv,i)

#calculate total rate of reactive power input
dQ = dqin + dq_elec - dqout
```

Figure 4-6: Using Numpy calculate rate of reactive power flow in Chiller

```
def derivate_spline(x,y):
    #calculate spline of data
    spl = UnivariateSpline(x, y, k=4, s=0)

    #calculate derivative of the spline
    d_spl = spl.derivative()

    #return the differentiated data
    return np.array([d_spl(t) for t in x])
```

(a) Differentiation using splines in Python

```
def energy_integrate(tau):
    #calculate spline of total power input
    P_spline = UnivariateSpline(t, P, k=4, s=0)

    #Firt fundamental equation of energy space
    def e_ode(y,t):
        return P_spline(t)-y/tau

    #Integrate ODE to calculate stored energy
    e = np.ndarray.flatten(integrate.odeint(e_ode,0,t))

    return e
```

(b) Integration using odeint in Python

Figure 4-7: Differentiation and Integration in Python

We then use the data generated using *Numpy* to calculate the differentiated and integrated values of the different interface variables. We use the spline functionality of *Statistics* module to first calculate a smooth spline of the data and use the spline to generate the derivatives at the given time instant. This approach introduces less error

in the calculated derivatives than using difference methods to calculate derivatives. We also use the ODE integration functionality of *Statistics* package to integrate the data with respect to time. An example of these functionality can be seen in Fig. 4-7.

Once, we have calculate all the desired interface variables and values of stored energy and energy in tangent space using the above mentioned methods, we can easily compare these values to verify the chiller model in energy-space.

Chapter 5

Results

5.1 Distributed Parameter Estimation

In this section, we show the numerical results of our distributed parameter estimation approach using measurements from a real industrial HVAC system under the assumption of weak coupling between each subsystem. As mentioned in the previous section, We use MATLAB's system identification toolbox to estimate the parameters over the measurement data to see how closely we can map the dynamics of the chiller. We train the model on the first 5 days of data and validate the model on the next 2 days of data.

5.1.1 Chiller Subsystem Identification

Based on the approach mentioned in Section 3.5, we estimate the critical parameters of the chiller model equation 3.2. The estimated parameters of the chiller subsystem can be seen in Table 5.1.

Parameter	Value (SI units)
α_1	6.60×10^{-5}
α_2	2.3568×10^{-10}
α_3	4.27×10^{-3}
α_4	1.2344

Table 5.1: Estimated Chiller Subsystem Parameters [33]

Based on the estimated parameters, we found the time constant of the chiller to be on the order of 20 minutes. This also agrees with experimental data.

The untrained model has a mean-squared (MSE) error as shown in equation 3.45 is 56. After 500 iterations of the estimation algorithm, we get a decent fit of the actual dynamics of the chiller with an MSE of 0.3 [33]. The comparison of the estimated parameters with actual data before and after the estimation algorithm can be seen Fig. 5-1 (a) and (b) respectively.

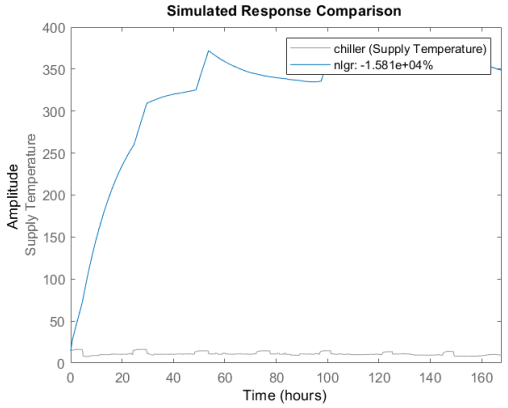

(a) Untrained Chiller model simulation

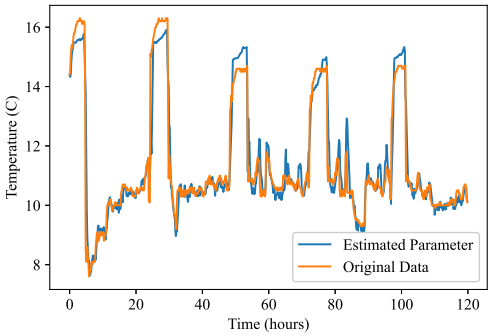

(b) Trained chiller model simulation

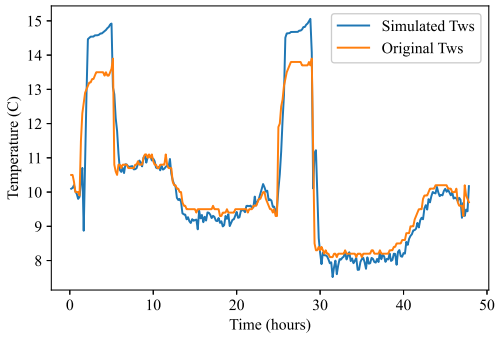

(c) Chiller model simulation vs validation data

Figure 5-1: Chiller Model Parameter Estimation [33]

We use the parameters shown in Table 5.1 and original control input to simulate the chiller model for the next two days. We can see a comparison of the simulated and actual measurement data for the supply temperature T_{ws} in Fig. 5-1 (c). The correlation between the simulated temperature $\hat{T}_{ws}$ and measured temperature T_{ws}

was 95.2% and the CV(RMSD) was 3.8% [33]. This further validates our parameter estimation for the chiller subsystem.

5.1.2 Pump Subsystem Identification

As shown in equation 3.11, 3.13 and 3.12, the state variables of the pump subsystem are the rotational frequency N_p, armature current I_p and water mass flow rate $\dot{m}_w$. The time constants for all the state variables are smaller than 10 minutes and the sampling rate for the measurement data is 10 minutes. The pump control is also bang-bang control as mentioned in Section 3.4.1. Therefore, we do not observe any transients in our measurement data. This decreases the accuracy of our parameter estimation results.

Therefore, we focus on the slower changes in the pump state variables at the quasi-steady state to estimate the pump model parameters. We only consider the data when the pump is ON and ignore the rest of the data. We also have some missing data samples between hours 50 and 100 as can be seen in Fig 5-2 (b).

The results of the parameter estimation for the pump model can be seen in Table 5.2. The comparison of the simulated mass flow rate $\hat{\dot{m}}_w$ with actual data $\dot{m}_w$ before and after the estimation algorithm can be seen Fig. 5-2 (a) and (b) respectively.

Parameter	Expression	Value (SI units)
β_1	$\frac{k_i}{2\pi J_p}$	0.0028
β_2	$\frac{B_p}{J_p}$	0.0105
β_3	h_{13}	2.3566×10^{-9}
β_4	$\frac{R_{a,p}}{L_{a,p}}$	0.0560
β_5	$\frac{2\pi k_{b,p}}{L_{a,p}}$	0.0737
β_6	$\frac{e_{a,p}}{L_{a,p}}$	0.0762
β_7	$\frac{1}{2}h_{31}$	4.835×10^{-6}
β_8	$\frac{1}{2}h_{33}$	7.5211×10^{-8}

Table 5.2: Estimated Pump Subsystem Parameters [33]

he model was then simulated for the next 2 days using the learned parameters in Table 5.2. The comparison of the simulated and actual mass flow rate data can be seen in Fig. 5-2 (c). The simulated data achieved a correlation of 80% and CV(RMSD)

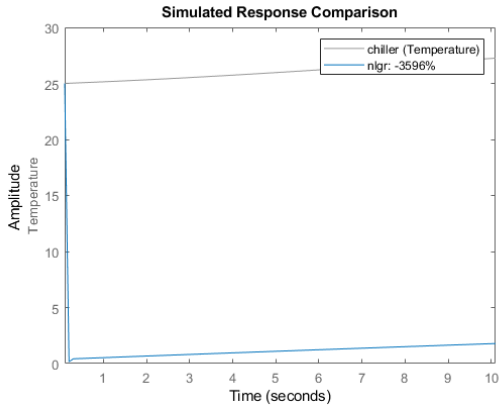

(a) Untrained water pump model

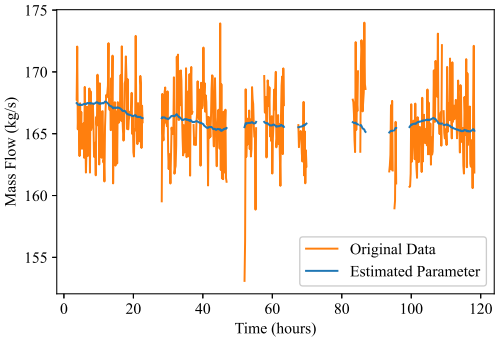

(b) Trained water pump model

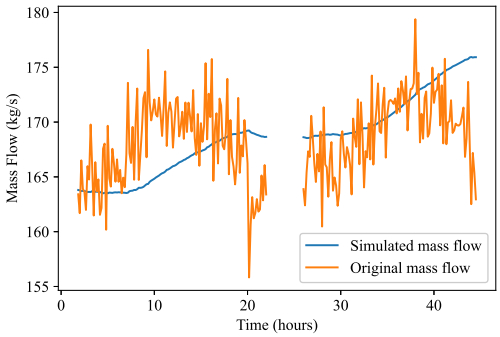

(c) Pump model simulation vs validation data

Figure 5-2: Pump model Parameter Estimation [33]

of 4.6% with the actual data [33]. We consider this an acceptable validation performance because we suspect the decrease in accuracy occurs due to the noise in the measurement data which can be seen in Fig. 5-2 and the low sampling rate of the measurement data relative to the time constant of the system.

Finally, in Section 3.4.1, our Assumption 2 stated that the natural responses of the states I_p and N_p of the pump are much faster than the natural response of other internal state, water mass flow $\dot{m}_w$. From the estimated parameters in Table 5.2, we can calculate the natural time constants of all the state variables of pump model. The time constant reciprocal for N_p is $\beta_2 + \beta_3 \approx 0.0105$. The time constant reciprocal for I_p is $\beta_4 = 0.056$. The time constant reciprocal for is $2\beta_8 \approx 2.55 \times 10^{-5}$ [33]. Therefore, the natural response of $\dot{m}_w$ is much slower than N_p and I_p, which confirms

Assumption-2.

5.2 Energy Space Model Verification

In this section, we verify the energy-space model of the chiller subsystem proposed in Section 3.6 using actual measurement data. For the chiller subsystem, mass flow rate $\dot{m}_w$, temperature at the output of chiller T_{ws}, the return water temperature T_{wr}, which enters chiller, and the water pressure at the input Pr_{ci} and output of the chiller Pr_{co}, are measured over seven days duration at the sampling rate of 10 minutes each as can also be seen in Fig. 5-3. This data set is divided into ON and OFF duration of system operation. In a 24 hour day, typically the chiller is seen to be ON for 80 % time duration. It must be noted that stored energy in the chiller is zero when the system is turned OFF, as the mass flow rate in the system is zero.

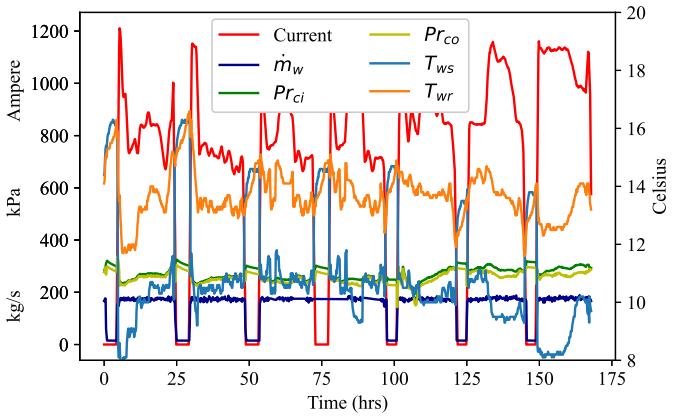

Figure 5-3: Available Chiller Measurements [14]

As a proof of concept, we will be validation the two fundamental equations of the energy-power space given by,

$$\dot{E} = P - \frac{E}{\tau} = p \tag{5.1}$$

$$\dot{p} = 4E_t - \dot{Q} \tag{5.2}$$

We explain the significance of these equations in detail in Section 2.4.2. We will

use the chiller measurement data to verify both these equation for the chiller energy-space model.

5.2.1 First Fundamental equation verification

To validate equation 5.1 using measurement data, we first calculate the total power input to the chiller subsytem P using the following equations [14]:

$$P_{pc}^{in} = c_w \dot{m}_w T_{wr} + (1/\rho_w)\dot{m}_w Pr_{ci} \tag{5.3}$$

$$P_{cs}^{out} = c_w \dot{m}_w T_{ws} + (1/\rho_w)\dot{m}_w Pr_{co} \tag{5.4}$$

$$P_{tc}^{in} = I_c V_c \tag{5.5}$$

$$P = P_{pc}^{in} + P_{tc}^{in} - P_{cs}^{out} \tag{5.6}$$

Then the stored energy E in the chiller is calculated using equation 5.1 as follows:

$$\dot{E} = P - \tfrac{E}{\tau} = p \tag{5.7}$$

The value of stored energy E are then verified by the value of E obtained from the thermodynamic equations for stored energy in the chiller given by [14]

$$E = C_w \times (T_{wr} - T_{ws}) \tag{5.8}$$

where, C_w is the thermal capacitance of the chiller.

We compare the value of stored energy calculated using 5.7 and 5.8 and see, if they are within our range of error. To quantify the model accuracy, the coefficient of variance of the root mean square deviation in the measured output is compared with the modelled output.

$$RMSD = \sqrt{\sum_{n=1}^{n=N}(y_p[n] - y_m[n])^2}/N \tag{5.9}$$

$$CV(RMSD) = RMSD/\bar{y}_p \tag{5.10}$$

where, $y_p[n]$ refers to the modelled value of the stored energy inside the chiller as computed from the data insertion in Eq. 5.7 and $y_m[n]$ shows the value of the stored energy evaluated by the measurement insertion in Eq. 5.8 [14].

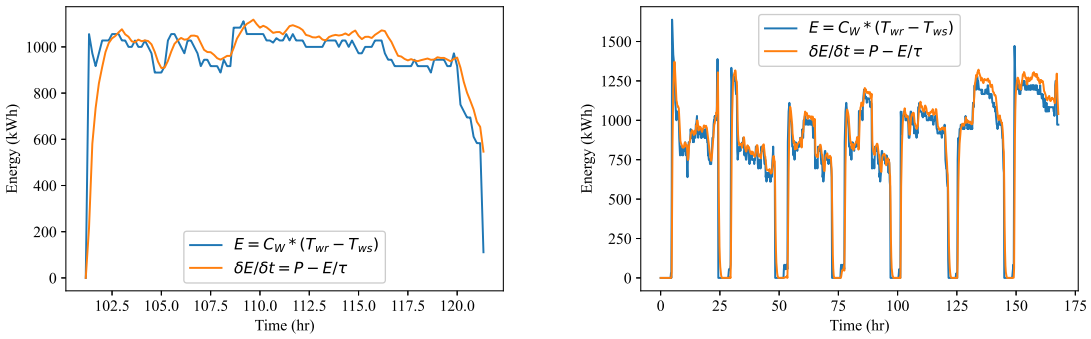

(a) Data for one ON duration

(b) Data for complete 7 days

Figure 5-4: Calculation of stored energy in chiller [14]

The comparison of the values of stored energy obtained from 5.7 and 5.8 can be seen in Fig. 5-4. Fig. 5-4 (a) shows the values of stored energy for one ON duration of the chiller which lasts about 18 hours and Fig. 5-4 (b) shows the comparison for all 7 days. The value of CV(RMSD) computed using 5.10 and correlation between the two values of stored energy calculated is [14]

$$CV(RMSD)(E) = 0.0108$$

$$Correlation(E) = 95.4$$

The calculated values of stored energy of the chiller using 5.7 and 5.8 show great agreement. Therefore, we have validated equation 5.1 for the chiller subsystem.

5.2.2 Second Fundamental Equation Verification

We verify the second fundamental equation in a way similar to the first fundamental equation shown in previous section. First we calculate the total rate of reactive power input to the chiller subsytem $\dot{Q}$ using the following equations [14]:

$$\dot{Q}^{in}_{pc} = c_w(\dot{m}_w T_{wr} - \dot{m}_w T_{wr}) + (1/\rho_w)(Pr_{ci}\dot{m}_w - \dot{m}_w Pr_{ci}) \quad (5.11)$$

$$\dot{Q}^{out}_{cs} = c_w(\dot{m}_w T_{ws} - \dot{m}_w T_{ws}) + (1/\rho_w)(Pr_{co}\dot{m}_w - \dot{m}_w Pr_{co}) \quad (5.12)$$

$$\dot{Q}^{in}_{tc} = V_c I_c T_{wr} - I_c V_c \quad (5.13)$$

$$\dot{Q} = \dot{Q}^{in}_{pc} + \dot{Q}^{in}_{tc} - \dot{Q}^{out}_{cs} \quad (5.14)$$

We also calculate the rate of change of stored energy p using the following equations:

$$p = \dot{E} \quad (5.15)$$

$$E = C_w \times (T_{wr} - T_{ws})$$

Then, the energy in tangent space E_t is calculated for the chiller using the energy-power space equation 5.2 as follows

$$E_t = (\dot{p} + \dot{Q})/4 \quad (5.16)$$

The value of E_t is also obtained from the fundamental thermodynamics equations for the chiller given by

$$E_t = (C_w/\tau) \times (\dot{T}_{wr} - \dot{T}_{ws}) \quad (5.17)$$

The comparison of the values of stored energy obtained from 5.16 and 5.17 can be seen in Fig. 5-5. Fig. 5-5 (a) shows the values of stored energy for one ON duration of the chiller which lasts about 18 hours and Fig. 5-5 (b) shows the comparison for

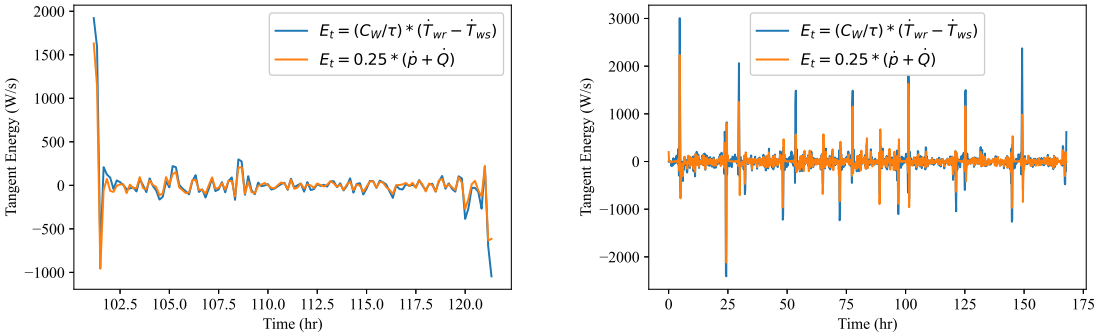

(a) Data for one ON duration

(b) Data for complete 7 days

Figure 5-5: Calculation of energy in tangent space for chiller [14]

all 7 days. The value of CV(RMSD) computed using 5.10 and correlation between the two values of energy in tangent space calculated is [14]

$$CV(RMSD)(E_t) = 0.0706$$

$$Correlation(E_t) = 92.1\%$$

We, thus, validate the second fundamental equation using chiller energy space model. Therefore, we have verified the energy-space modelling using measured data with high-accuracy.

5.2.3 Effects of Pressure

The reduced order dynamic equation for the chiller subsystem is given by equation 3.1. This equation guides the internal states of the chiller and since we see no dependence on the pressure, the dynamical model either neglects or assumes a constant effect of pressure on the internal states. Here, we show that the pressure change across the chiller is essential for verifying the the second fundamental equation 5.2 in energy space and is important accurately model the chiller subsystem.

We can see the pressure change measurement data across the chiller for 2 days in Fig. . The separate data for water pressure into and out of the chiller for entire 7

days can be seen in Fig. 5-3.

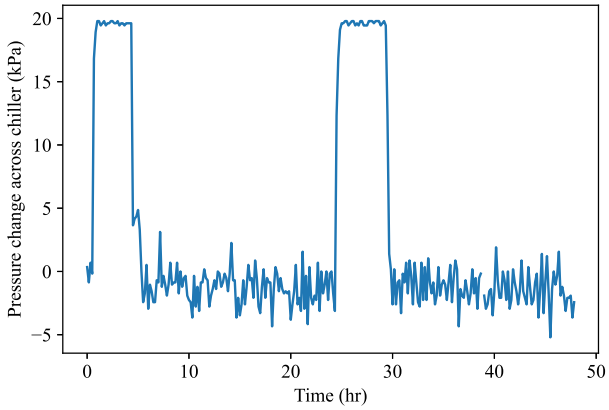

Figure 5-6: Pressure difference across chiller [14]

We first calculated the rate of reactive energy into the chiller $\dot{Q}$ without using the contributions from pressure of water or the effort variable as follows [14]

$$\dot{Q}_{pc}^{in} = c_w(\dot{m}_w T_{wr} - \dot{m}_w T_{wr}) \tag{5.18}$$

$$\dot{Q}_{cs}^{out} = c_w(\dot{m}_w T_{ws} - \dot{m}_w T_{ws}) \tag{5.19}$$

$$\dot{Q}_{tc}^{in} = V_c I_c T_{wr} - I_c V_c \tag{5.20}$$

$$\dot{Q} = \dot{Q}_{pc}^{in} + \dot{Q}_{tc}^{in} - \dot{Q}_{cs}^{out} \tag{5.21}$$

Using the values of $\dot{Q}$ obtained from equation 5.21 and the values of p obtained from equation 5.15 and substitute these values in equation 5.16.

The values of energy in tangent space then obtained using the above mentioned 5.16 and 5.17 can be seen in Fig. 5-7. Fig. 5-4 (a) shows the values of stored energy for one ON duration of the chiller which lasts about 18 hours and Fig. 5-4 (b) shows the comparison for all 7 days. The value of CV(RMSD) computed using 5.10 and correlation between the two values of stored energy calculated is

$$CV(RMSD)(E) = 1.16$$

$$Correlation(E) = -42\%$$

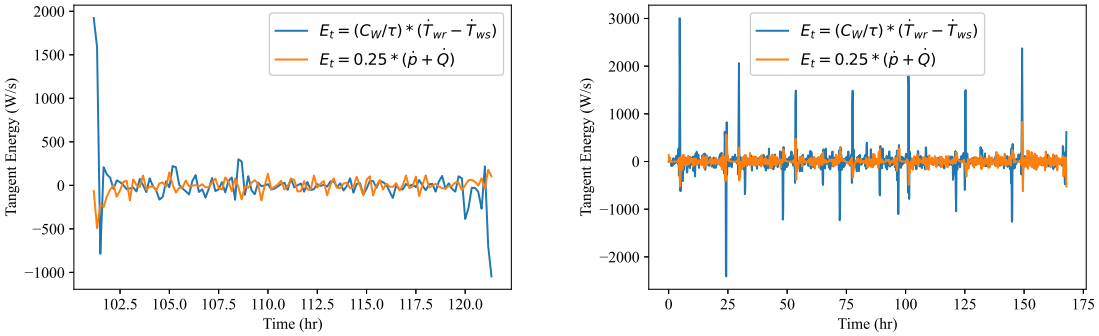

(a) Data for one ON duration

(b) Data for complete 7 days

Figure 5-7: Calculation of energy in tangent space for chiller without contribution of pressure [14]

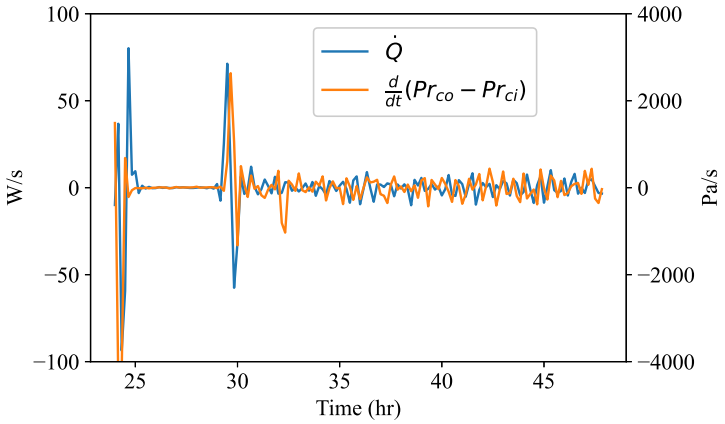

Figure 5-8: Correlation between $\dot{Q}$ and rate of change of pressure across chiller [14]

Thus, we can accurately calculate the value of E_t without taking into account the contribution of pressure change across the chiller or the contribution of effort variable in calculation of $\dot{Q}$. We can also see in Fig. , the comparison of $\dot{Q}$ calculated using 5.14 by taking into account pressure change and the rate of change of pressure difference across the chiller. We can conclude from Fig. that the contribution of effort variable in calculating the rate of reactive power is indeed essential.

We can see in Fig. 5-6, that the pressure change across the chiller is almost constant and close to zero (with some measurement noise) when the chiller is operational. Therefore, neglecting its contribution in the conventional state space model

of the chiller given by 3.1 does not introduce a lot error into the model. But using measurement data from a commercial chiller, we have verified that the contribution of pressure change across chiller is necessary for calculating the total reactive power into the chiller and thus, necessary for evaluating the inefficiencies in the system using energy-space model.

Chapter 6

Conclusion

6.1 Conclusion

In this thesis, we focused on problems that are important in designing efficient controls for a complex dynamical system in multi-energy domain. We use a commercial HVAC system since its complexity and multi-energy interactions provide a suitable exampel for analysing these problems first hand as well as testing our methodology.

Designing efficient control as well as more sophisticated models of the system require knowledge of the model parameters of the components. Researchers have often circumvented this problem by either using statistical relationships between control and state variables or by using simpler or static models. We have shown a distributed parameter estimation approach with low computational cost and using limited sensor measurements to work well for various components in the HVAC system. We decompose a weakly-coupled HVAC subsystem using diagonally dominant matrices. We also comment on the limits on the type of control that can be used to decompose such a system. For this result, we didnot install new sensors or generate data in a experimentally controlled setting. We verified our methodology using data which is available in most HVACs and during normal operating conditions. Therefore, we can use this approach to calculate parameters of models in real time without any extra overhead cost from new sensors or calibration time.

Advanced control algorithms require accurate representation of the system which

requires accurate models of the system. But due to the increasing complexity of these systems, the implementation often resorts to reduced order or static models of the system. It has been shown that these models are often not accurate enough and can not deal with fast-prone disturbances which are common in today's energy systems. Therefore, we modeled the HVAC system using a novel approach using effort and flow variables at the ports in energy-power space. Energy-power space model is a form of aggregate model which takes into account the power and reactive power inputs from the neighbours and thus reduces the complexity of the interconnected system. Here, we show how we can use sensor available in most HVACs in a real world setting to calculate the power and rate of reactive power flow in the system. We use the same data to verify the energy-power space model of an electric chiller at nearly 99% accuracy. A novel finding using the energy-space model is that unless we use both effort and flow variables at the interface, the rate of reactive power into a component cannot be accurately calculated. Conventional state space models often assume constant effort variables but effort variable in reality is not constant and is necessary in energy-power space to deal with fast responding disturbances.

While these results have primarily been posed and verified within the context of HVAC systems, they are valuable for designing control of any complex interconnected system comprising of multiple energy conversion processes.

6.2 Future Work

The work done in this thesis was intended to be used in next-generation Dynamic Monitoring and Decision Systems (DyMonDS) framework. DyMonDS leverages optimal minimal exchange wherein the agents exchange minimal information with their coordinators. This work can greatly aid the design of better control algorithms for HVAC systems using DyMonDS [16].

We only provide a proof-of-concept for the distributed parameter estimation approach mentioned in this thesis. The approach needs to be extended for other subsystems in the HVAC as well as needs to be scaled for bigger subsystems. Additionally,

we also need to compare the performance of the distributed parameter estimation with standard parameter estimation on a controller.

Finally, we were only able to design and verify the energy-space model for a single component of the HVAC system. DyMonDS and control in energy-power space for the HVAC will require multiple interconnected components to be modelled in the energy-power space. This is essential for proving higher energy efficiency gains using DyMonDS over the current control algorithms used in industrial HVACs.

Bibliography

[1] Grey-box model estimation. https://www.mathworks.com/help/ident/grey-box-model-estimation.html?s_tid=CRUX_lftnav. Accessed: 2020-07-30.

[2] idnlgrey. https://www.mathworks.com/help/ident/ref/idnlgrey.html. Accessed: 2020-07-30.

[3] nlgreyest. https://www.mathworks.com/help/ident/ref/nlgreyest.html. Accessed: 2020-07-30.

[4] nlgreyestoptions. https://www.mathworks.com/help/ident/ref/nlgreyestoptions.html. Accessed: 2020-07-30.

[5] Numpy. https://numpy.org/. Accessed: 2020-07-30.

[6] pandas. https://pandas.pydata.org/. Accessed: 2020-07-30.

[7] statistics. https://docs.python.org/3/library/statistics.html. Accessed: 2020-07-30.

[8] System identification toolbox. https://www.mathworks.com/products/sysid.html. Accessed: 2020-07-30.

[9] *2008 ASHRAE handbook: heating, ventilating, and air-conditioning systems and equipment*. American Society of Heating, Refrigerating, and Air-Conditioning Engineers, 2008.

[10] Model predictive hvac load control in buildings using real-time electricity pricing. *Energy and Buildings*, 60:199 – 209, 2013.

[11] Theory and applications of hvac control systems – a review of model predictive control (mpc). *Building and Environment*, 72:343 – 355, 2014.

[12] A. Beghi and Luca Cecchinato. Modelling and adaptive control of small capacity chillers for hvac applications, Dec 2010.

[13] W.h. Bennett and J.s. Baras. Block diagonal dominance and design of decentralized compensators. *IFAC Proceedings Volumes*, 13(6):93–101, 1980.

[14] Pallavi Bharadwaj, Janak Agrawal, Rupamathi Jaddivada, Min Zhang, and Marija Ilic. Measurement based validation of energy-space modelling in multi-energy systems. *North American Power Symposium (NAPS)*, 2020 (To be reviewed).

[15] S. Bittanti, A. De Marco, M. Giannatempo, and V. Prandoni. A dynamic model of an absorption chiller for air conditioning. *Renewable Energy and Power Quality Journal*, 1(08):643–648, 2010.

[16] Ilic Marija D. Toward a unified modeling and control for sustainable and resilient electric energy system. *Foundations and Trends® in Electric Energy Systems*, 1(1):1–141, 2016.

[17] David G. Feingold and Richard Varga. Block diagonally dominant matrices and generalizations of the gerschgorin circle theorem. *Pacific Journal of Mathematics*, 12(4):1241–1250, 1962.

[18] Miroslav Fiedler and Vlastimil Pták. Diagonally dominant matrices. *Czechoslovak Mathematical Journal*, 17(3):420–433, 1967.

[19] Hannah Friedman, Portland Energy Conservation, and Inc Priya Sreedharan. Wiring the smart grid for energy savings: mechanisms and policy considerations. *ACEEE Summer Study Energy Eff Build*, 2010.

[20] Natarajkumar Hariharan and Bryan P Rasmussen. Parameter estimation for dynamic hvac models with limited sensor information. *INFONA*.

[21] Marija Ilic and Rupamathi Jaddivada. Toward technically feasible and economically efficient integration of distributed energy resources. In *2019 57th Annual Allerton Conference on Communication, Control, and Computing (Allerton)*, pages 796–803. IEEE, 2019.

[22] Marija Ilic and Rupamathi Jaddivada. Unified value-based feedback, optimization and risk management in complex electric energy systems. *Optimization and Engineering*, pages 1–57, 2020.

[23] Marija D Ilic and Rupamathi Jaddivada. Multi-layered interactive energy space modeling for near-optimal electrification of terrestrial, shipboard and aircraft systems. *Annual Reviews in Control*, 45:52–75, 2018.

[24] Marija D Ilic and Rupamathi Jaddivada. Exergy/energy dynamics-based integrative modeling and control for difficult hybrid aircraft missions. *AIAA Propulsion and Energy 2019 Forum*, page 4501, 2019.

[25] Marija D Ilic and Rupamathi Jaddivada. Novel modeling and control for maximizing efficiency of hvacs participating in fast ancillary services. *White Paper*, 2020.

[26] J. Jazaeri, T. Alpcan, and R. L. Gordon. A joint electrical and thermodynamic approach to hvac load control. *IEEE Transactions on Smart Grid*, 11(1):15–25, 2020.

[27] B. T. Lopez and J. E. Slotine. Adaptive nonlinear control with contraction metrics. *IEEE Control Systems Letters*, pages 1–1, 2020.

[28] Oliver Nelles. *Nonlinear System Identification - From Classical Approaches to Neural Networks and Fuzzy Models: Oliver Nelles.* Springer-Verlag Berlin Heidelberg.

[29] Matthew Overlin, Christopher Smith, Marija Ilic, and James L. Kirtley. A workflow for non-linear load parameter estimation using a power-hardware-in-the-loop experimental testbed. *2020 IEEE Applied Power Electronics Conference and Exposition (APEC)*, 2020.

[30] Anders Rantzer. Distributed control of positive systems. In *2011 50th IEEE Conference on Decision and Control and European Control Conference*, pages 6608–6611. IEEE, 2011.

[31] Dragoslav D Šiljak and AI Zečević. Control of large-scale systems: Beyond decentralized feedback. *Annual Reviews in Control*, 29(2):169–179, 2005.

[32] Herbert W. III Stanford. *HVAC Water Chillers and Cooling Towers: Fundamentals, Application, and Operation.* CRC Press, 2017.

[33] Dan Wu, Janak Agrawal, Pallavi Bharadwaj, Le Li, Jinyi Zhang, and Marija Ilic. Measurement based validation of energy-space modelling in multi-energy systems. *North American Power Symposium (NAPS)*, 2020 (To be reviewed).

[34] FW Yu and KT Chan. Optimization of water-cooled chiller system with load-based speed control. *Applied Energy*, 85(10):931–950, 2008.

[35] FW Yu and KT Chan. Environmental performance and economic analysis of all-variable speed chiller systems with load-based speed control. *Applied Thermal Engineering*, 29(8-9):1721–1729, 2009.

[36] X. Zhang, M. Pipattanasomporn, T. Chen, and S. Rahman. An iot-based thermal model learning framework for smart buildings. *IEEE Internet of Things Journal*, 7(1):518–527, 2020.

[37] Zhang Huaguang and Lilong Cai. Decentralized nonlinear adaptive control of an hvac system. *IEEE Transactions on Systems, Man, and Cybernetics, Part C (Applications and Reviews)*, 32(4):493–498, 2002.

[38] Guo Rong Zheng. *Dynamic modeling and global optimal operation of multizone variable air volume HVAC systems.* PhD thesis, Concordia University, 1997.